2014

Cosmological And Astrophysical Tests Of Modified Gravity

Caixia Gao
University of Mississippi

COSMOLOGICAL AND ASTROPHYSICAL TESTS OF MODIFIED GRAVITY

Caixia Gao

A dissertation presented for the Doctor of Philosophy degree

Department of Physics

University of Mississippi

December, 2014

Abstract

Three alternative theories to General Relativity will be studied. The aim is to test these theories by applying them to astronomical objects or the cosmological background. The first one is unimodular relativity. The cosmological perturbation theory of this model is studied and the predictions on temperature fluctuations of the CMB are found. The second one is dRGT massive gravity. In this theory a charged black hole solution is found and compared to those in GR, followed by constraints on the parameter space. The third one is a general massive gravity theory which shares the same background equation with the massless case except the evolution equation for the tensor perturbations. The signature of the graviton mass on the CMB polarization spectrum will be studied. A moderate graviton mass (comparable to the Hubble rate during recombination) leads to interesting modifications on the B mode polarization power spectrum. A large graviton mass is found to suppress the spectrum, therefore a tight constraint on the graviton mass can be found.

Dedication

To my parents

Enu Fan and Fengrong Gao

Acknowledgments

I am heartily thankful to my parents and my brothers whose supports and understanding enabled me to pursue my dream.

I am very grateful to my supervisor, Luca Bombelli, whose guidance, patience, and encouragements enabled me to develop an understanding of the subject.

I am very grateful to Yifu Cai and Robert Brandenberger for stimulating discussions, interesting collaborations and constant encouragements.

I am thankful to Raphael Flauger and David Sanders for helping me out debugging and running programs.

I am thankful to Emanuele Berti, Alakabha Datta and Erwin Mina Diaz for helpful questions and comments.

I express my deep gratitude to the Department of Physics and Astronomy at Ole miss for their long time supports. I am thankful to all faculty members for courses they taught me. I owe my sincere gratitude to Thomas Jamerson for his great help when I was teaching the Engineering labs.

Table of Contents

List of Figures

Figure Number Page

Chapter 1

INTRODUCTION

Current astronomical observations show that the expansion rate of the universe is accelerating. This was first discovered in 1998 by the High-z Supernova Search Team and the Supernova Cosmological Project [86, 88]. To explain this acceleration, General Relativity (GR) introduces a cosmological constant Λ. This is equivalent to introducing a new matter or energy with energy-momentum tensor proportional to the metric $T_{\mu\nu} = -\rho_\Lambda g_{\mu\nu}$, where $\rho_\Lambda = \frac{\Lambda}{8\pi G}$ is the constant energy density. Then any energy of this form will gravitate in the same way as regular matter, such as dark energy or the vacuum energy from Quantum Field Theory (QFT). The value of Λ is not set from the GR structure. On one hand, observations from the supernova search indicate that the acceleration of our universe is consistent with a positive cosmological constant,

$$\rho_\Lambda = 8.611 \times 10^{-30} \mathrm{g/cm}^3. \tag{1.1}$$

This is from the recent data released by the Planck collaboration [1]. On the other hand, the estimation from QFT is more than 120 orders of magnitude larger than this experimental bound. Then the question is, why is the vacuum energy so small now? This is the cosmological constant problem.

Many alternative gravity theories to GR [32], such as $f(R)$ theories in which the scalar Lagrangian R is generalized to a function $f(R)$ [36], $f(T)$ theories, which works in the tetrad framework and the torsion scalar T is generalized to a function $f(T)$ [64], Galileon gravity, in which the field Lagrangian is restricted to satisfy the Galilean symmetry in the Minkowski spacetime [31, 94], have claimed to be able to solve this problem. In these projects I will

focus on three of these: unimodular relativity, dRGT massive gravity and general massive gravity.

1.1 Unimodular relativity

Unimodular Relativity (UR) is an alternative theory of gravity first considered by Einstein in 1919 [46] and put into action form by Anderson and Finkelstein in 1991 [50]. The basic idea is that the determinant of the metric is a fixed density $\mu(x)$ and is to be determined by experiments. Then the field equation of motion will be the trace-free Einstein field equation. Therefore any energy-momentum of the form $T_{\mu\nu} = -\rho_\Lambda g_{\mu\nu}$ won't gravitate. This includes the cosmological constant and the vacuum energy. Although it seems that there is one less equation than in GR, the full Einstein field equation can be recovered by integration as long as the continuity equation is satisfied. The cosmological constant appears as an integration constant, which is determined by initial conditions and is independent of the vacuum energy. Thus UR avoids the cosmological constant problem. Lots of studies have been done in both classical ways and quantum ways so far [18, 20, 63, 84, 96, 102]. It is worth to mention that the quantization of UR also resolves the problem of defining a physically meaningful time with which to measure evolution of quantum states in quantum cosmology in the absence of a spatial boundary [21, 96, 97]. Classically, since the Einstein field equation can be recovered from the trace-free Einstein field equation [47], it is widely accepted that UR is indistinguishable from GR. However, GR is diffeomorphism-invariant while in UR the diffeomorphism gauge group is broken, and only the unimodular gauge transformations, those which satisfy $g^{\mu\nu}\delta g_{\mu\nu} = 0$, are allowed. We expect that this may make them different in the context of cosmological inhomogeneities. The aim of this project is to test UR by studying the cosmological perturbations.

1.2 dRGT massive gravity

Massive gravity is another way to modify GR by giving the graviton a mass. It was first initiated in 1939 by Fierz and Pauli (FP) and the corresponding Fierz-Pauli action they used is given by [49]

$$L = L_{\rm EH}(h) + m^2(h_{\mu\nu}h^{\mu\nu} - h^2), \tag{1.2}$$

where $L_{\rm EH}(h)$ is the linearized Einstein Hilbert action, m is the mass of the graviton and $h_{\mu\nu}$ is the perturbation of the metric, $g_{\mu\nu} = \eta_{\mu\nu} + h_{\mu\nu}$ with $\eta_{\mu\nu}$ is the Minkowski metric. Because of the mass term added, the diffeomorphism invariance is broken in this action. It describes a massive spin-2 graviton with 5 degrees of freedom, 2 tensor modes, 2 vector modes and 1 scalar mode. It is the unique Lorentz invariant massive gravity theory at linear order without ghosts [105].

However, it was found in the 1970s that this linearized theory can not be reduced to GR in the limit of vanishing graviton mass; this is known as the van Dam-Veltman-Zakharov (vDVZ) discontinuity [104, 110]. Consequently, some observables will show a discontinuity in the massless limit. For example, the light bending is off by 25 percent from the GR prediction. As a result, it seems that massive gravity can be easily ruled out by experiments in our solar system. Later this was traced to the longitudinal mode of the graviton, which is coupled with the trace of the energy momentum tensor even though the mass goes to zero [39].

Later Vainshtein found that this troublesome mode can be screened by including non-linear effects and GR can be recovered within the Vainshtein radius [103], $r_V = (\frac{GM}{m^4})^{1/5}$. Within this radius, non-linearities dominate and predictions of linear theories can not be trusted. The Vainshtein radius is usually very large and it goes to infinity as m approaches 0. So we can not rule out this theory that easily.

Although non-linear effects cure the discontinuity, the Hamiltonian constraint gets lost and as a result, the theory has 6 degrees of freedom now instead of 5 as in the original linear theory. This extra degree of freedom manifests itself as a scalar field with a wrong sign kinetic term, which is the Boulware-Deser (BD) ghost [22], and this non-linear theory is thus unstable [3].

In order to avoid the ghost instability and maintain the Vainshtein mechanism, a family of non-linear ghost-free massive gravity theories was proposed by de Rham, Gabadadze and Tolley (dRGT) in 2010. The cosmological and black hole solutions of this theory have been studied very well so far [5, 6, 7, 13, 24, 29, 33, 55, 69, 71, 72, 79, 85, 91, 95, 106]. Although some of the black hole solutions are found to be unstable under perturbations or

discharge process [5, 8, 24, 79, 80], however these are model dependent and their background solutions are exactly the same as GR. In my project, the charge black hole solution has higher order corrections on the Reissner-Nordstrom black hole solution in GR except one particular parameter choice. Since the scalar field, which causes the vDVZ discontinuity, is coupled to the energy momentum, we are expecting that the electromagnetic field may have an effect on the Vaishtein mechanism. The aim of this project is to find the constraints on dRGT massive gravity by studying the charged black hole solutions.

1.3 Lorentz breaking massive gravity

Both the FP massive gravity and the dRGT massive gravity are Lorentz invariant in the Minkowskian background. Although dRGT massive gravity can evade the vDVZ discontinuity by the Vainshtein mechanism, it does not have a spatially flat FRW universe solution, and the perturbations of open FRW universes are not stable. It was realized that Lorentz breaking massive gravity theories may soften these problems [89]. Instead of requiring the full Lorentz invariance, only rotational invariance is preserved. Depending on the parameter choice, the minimum modification to GR would be that they share the same background evolution equation with GR as well as the evolution of scalar and vector perturbations, the only modification is the tensor mode whose dispersion relation takes the form $\omega^2 = k^2 + m_g^2$. Therefore the speed of gravitational waves, which is less than speed of light, depends on the graviton mass. This will lead to different observations for supernovae, inspiralling compact binaries and the cosmic microwave background from those in GR. Hence, constraints on graviton mass can be found by observing the behavior of gravitational waves in these systems [14, 15, 19, 24, 30, 51, 73, 78, 98, 99, 108, 109]. In this project we will study the effect of graviton mass on CMB power spectra.

Chapter 2

PROJECT I: COSMOLOGICAL PERTURBATIONS OF UNIMODULAR RELATIVITY

2.1 The action form of unimodular relativity

We take the action proposed by Anderson and Finkelstein [50]

$$S = \int d^4x\sqrt{-g}\left[\frac{1}{16\pi G}R + \frac{1}{16\pi G}\chi\Big(1 - \frac{\mu(x)}{\sqrt{-g}}\Big) + \mathcal{L}_m\right] \ , \tag{2.1}$$

where G is the gravitational constant, R is the Ricci scalar of the physical metric $g_{\mu\nu}$, $\mathcal{L}_m$ is the Lagrangian for matter fields, χ is a Lagrangian multiplier and $\mu(x)$ is a fixed scalar density.

The variation with respect to χ gives a constraint on the metric:

$$\sqrt{-g} = \mu(x). \tag{2.2}$$

The variation with respect to the metric gives the field equation

$$R_{\mu\nu} - \frac{R}{2}g_{\mu\nu} - \frac{\chi}{2}g_{\mu\nu} = 8\pi G T_{\mu\nu} \ , \tag{2.3}$$

where $T_{\mu\nu}$ is the energy-momentum tensor for matter, defined as $T_{\mu\nu} \equiv -\frac{\delta(\sqrt{-g}\mathcal{L}_m)}{\sqrt{-g}\delta g^{\mu\nu}}$, which is the same as that in GR.

Taking the trace of (2.3) gives the Lagrange multiplier:

$$\chi = -\frac{1}{2}\Big(R + 8\pi G\, T\Big) \ , \tag{2.4}$$

where $T \equiv T^{\mu}_{\mu}$ is the trace of the energy momentum tensor. Substituting the above equation into (2.3), we obtain the trace-free Einstein field equation

$$\hat{G}_{\mu\nu} = 8\pi G \hat{T}_{\mu\nu} \ , \tag{2.5}$$

with

$$\hat{G}_{\mu\nu} := R_{\mu\nu} - \frac{R}{4} g_{\mu\nu} \ , \quad \hat{T}_{\mu\nu} := T_{\mu\nu} - \frac{T}{4} g_{\mu\nu} \ . \tag{2.6}$$

The covariant divergence of (2.5) is

$$\nabla_{\mu} T^{\mu\nu} = \frac{1}{4} g^{\mu\nu} \nabla_{\mu} (R + {M_p}^{-2} T) = -\frac{1}{2} g^{\mu\nu} \nabla_{\mu} \chi, \tag{2.7}$$

where the Bianchi identity has been applied. Therefore, the energy-momentum conservation equation,$\nabla_{\mu} T^{\mu\nu} = 0$, is not an identity in unimodular relativity. However, this condition is always satisfied by the virtue of the field equation for matter that we know now. Then in unimodular relativity this condition has to be imposed as an assumption. If we follow this assumption, then the undetermined multiplier χ can be identified with a cosmological constant Λ. Therefore the Einstein field equation is recovered [47, 107]

$$R_{\mu\nu} - \frac{1}{2} g_{\mu\nu} R - \Lambda g_{\mu\nu} = 8\pi G T_{\mu\nu}. \tag{2.8}$$

In the next two sections, we will first consider a universe filled with a single scalar field, then do a similar analysis for a universe filled with hydrodynamical matter.

2.2 Cosmological perturbation with a scalar field

On one hand, inflation provides a mechanism for producing the primordial density perturbations and predicts a scale-invariant anisotropy of the Cosmic Microwave Background (CMB), which agrees well with current observations. The simplest inflationary model is driven by a single scalar field, and this is also the preferred model according to the Planck collaboration data [1]. On the other hand, at very high energy, we expect that matter will

be described in terms of fields. Therefore in this chapter we will work out the cosmological perturbations for a single scalar field φ, with Lagrangian given by

$$\mathcal{L}_m = \frac{1}{2}\nabla_\mu\varphi\nabla^\mu\varphi - V(\varphi) \ , \tag{2.9}$$

with V being the field potential. The corresponding equation of motion is the Klein-Gordon equation:

$$\nabla_\mu\nabla^\mu\varphi + V_{,\varphi} = 0 \ , \tag{2.10}$$

where $V_{,\varphi}$ denotes the derivative of the scalar field potential with respect to φ.

2.2.1 FRW Background

We choose the background metric to be the Friedmann-Robertson-Walker (FRW) metric,

$$ds^2 \ = \ dt^2 - a^2(t)\gamma_{ij}dx^i dx^j \ = \ a^2(\eta)(d\eta^2 - \gamma_{ij}dx^i dx^j), \tag{2.11}$$

where η is the conformal time $d\eta = a^{-1}dt$, x^i are the comoving spatial coordinates and $\gamma_{ij} = \delta_{ij}[1+\frac{1}{4}k(x^2+y^2+z^2)]^{-2}$ with $k = 0, 1, -1$ depending on whether the three-dimensional space is flat, closed or open. In the following, we will just focus on the flat case since it is easy to extend the analysis to the general case.

In this chapter instead of starting with the Einstein field equation, we will start with the trace-free field equation (2.5). On the FRW background, there are two equations including the scalar field equation,

$$\mathcal{H}^2 - \mathcal{H}' = 4\pi G\varphi'^2, \tag{2.12}$$

$$\varphi'' + 2\mathcal{H}\varphi' + a^2V_{,\varphi} = 0, \tag{2.13}$$

where $\mathcal{H} = a'/a$ using conformal time. In contrast, GR has one more equation,

$$\mathcal{H}' + 2\mathcal{H}^2 = 8\pi G a^2 V(\varphi). \tag{2.14}$$

However, it can be proved directly by integration that the first two equations imply the third one. Therefore, on the FRW background the field equations in UR are equivalent to those in GR.

2.2.2 Scalar perturbations

A general metric perturbation can be categorized into three types: scalar, vector and tensor perturbations [76]. This refers to the way they transform under three-space coordinate transformations on the constant time hypersurface. Vector perturbations decay in an expanding universe whereas tensor perturbations lead to gravitational waves. Scalar perturbations may lead to growing inhomogeneities and play important roles on the dynamics of matter [16]. Therefore in this project we only consider the scalar metric perturbations [82],

$$ds^2 = a^2(\eta)\left[\,(1+2\phi)dt^2 - 2B_{;i}dx^i d\eta - ((1-2\psi)\gamma_{ij} + 2E_{;ij})dx^i dx^j\,\right], \tag{2.15}$$

where the semicolon denotes the three-dimensional covariant derivative. The scalar metric fluctuations are characterized by four functions ϕ, ψ, B, E which depend on both space and time.

The perturbation of the scalar field is given by $\varphi = \varphi(t) + \delta\varphi(t, x^i)$. Here we assume an isotropic background. The perturbed Einstein equation for unimodular relativity is derived from the field equation 2.5 and takes the form

$$\delta\hat{G}^{\mu}_{\nu} = 8\pi G\delta\hat{T}^{\mu}_{\nu}\ . \tag{2.16}$$

From the above equations and the perturbed metric, the non-vanishing perturbed equations of motion are given by the following,

$$\psi'' + \mathcal{H}(\phi-\psi)' + \frac{1}{3}\nabla^2[\phi + 2\psi - \mathcal{H}(B-E') + (B-E')'] = 8\pi G\varphi'\delta\varphi', \tag{2.17}$$

$$\psi'' + \mathcal{H}(\phi-\psi)' + \nabla^2[\phi + \mathcal{H}(B-E') + (B-E')'] - 2D_{,ii} = 8\pi G\varphi'\delta\varphi', \tag{2.18}$$

$$(\psi' + \mathcal{H}\phi)_{;i} = 4\pi G\varphi'\delta\varphi_{;i}, \tag{2.19}$$

$$D_{;ij} = 0, \tag{2.20}$$

where $D = \phi - \psi + 2\mathcal{H}(B - E') + B' - E''$ and ∇^2 is the Laplacian operator on the constant time hypersurface. The above perturbation equations correspond to the (00), (ii), $(0i)$ and (ij) (off diagonal) components, respectively. One can see that the potential of the scalar field does not show up in the metric equations, as it does in GR, so it may seem that the potential does not have any effect on the geometry. However, this is not true. From the perturbed Klein-Gordon equation:

$$\begin{aligned} &\delta\varphi'' + 2\mathcal{H}\delta\varphi' - \nabla^2\delta\varphi + a^2 V_{,\varphi\varphi}\delta\varphi - \varphi'(\phi + 3\psi)' \\ &+ 2a^2 V_{,\varphi}\phi - \varphi'\nabla^2(B - E') = 0, \end{aligned} \tag{2.21}$$

we can see that the potential will influence the geometry through the scalar field equation.

With respect to GR, there is an extra constraint for UR due to the fixed determinant of the metric, $g^{\mu\nu}\delta g_{\mu\nu} = 0$,

$$\nabla^2 E + \phi - 3\psi = 0. \tag{2.22}$$

As we will find later, this constraint is actually very strong on the perturbations.

2.2.3 Gauge freedom

Since we are only considering the scalar metric perturbations now, we will just focus on those diffeomorphisms which preserve the scalar nature of the metric fluctuations. The most general ones can be described by two functions ξ^0 and ξ,

$$\eta \to \tilde{\eta} = \eta + \xi^0(\eta, \vec{x}), \quad x^i \to \tilde{x}^i = x^i + \gamma^{ij}\xi_{,j}(\eta, \vec{x})\,.$$

In GR, the gauge group is the diffeomorphism group, and ξ^0 and ξ are independent functions. However, in unimodular gravity, since only the unimodular gauge transformations are allowed, the two parameters are related to each other 2.22,

$$\nabla^2\xi + \xi^{0\prime} + 4\mathcal{H}\xi^0 = 0. \tag{2.23}$$

To fix a gauge, this condition has to be satisfied. This transformation induces a change in the metric variables, the new perturbations being given by

$$\tilde{\phi} = \phi - (a'/a)\xi^0 - \xi^{0\prime},\ \tilde{\psi} = \psi + (a'/a)\xi^0,$$
$$\tilde{B} = B + \xi^0 - \xi',\ \ \tilde{E} = E - \xi. \tag{2.24}$$

Neither $\delta\hat{G}^{\mu}_{\nu}$ nor $\delta\hat{T}^{\mu}_{\nu}$ are gauge-invariant. It turns out that they transform in the same manner. We will just list the transformation laws for one of them here,

$$\delta\hat{G}^0_0 \to \delta\hat{G}^0_0 - ({}^{(0)}\hat{G}^0_0)'\xi^0,$$
$$\delta\hat{G}^0_i \to \delta\hat{G}^0_i - \Big({}^{(0)}\hat{G}^0_0 - \frac{1}{3}{}^{(0)}\hat{G}^k_k\Big)\xi^0_{,i},$$
$$\delta\hat{G}^i_j \to \delta\hat{G}^i_j - ({}^{(0)}\hat{G}^i_j)'\xi^0. \tag{2.25}$$

However, we can always choose gauge-invariant variables. There are many ways to do this. For the metric perturbations, the simplest choice would be to introduce

$$\Phi = \phi + (1/a)[(B - E')a]',\ \ \Psi = \psi - (a'/a)(B - E'),$$

while for the gauge-invariant variables $\delta\hat{G}^{(\mathrm{gi})\alpha}_{\beta}$ we will choose

$$\delta\hat{G}^{(\mathrm{gi})0}_0 = \delta\hat{G}^0_0 + ({}^{(0)}\hat{G}^0_0)'(B - E')$$
$$\delta\hat{G}^{(\mathrm{gi})0}_i = \delta\hat{G}^0_i + ({}^{(0)}\hat{G}^0_0 - \frac{1}{3}{}^{(0)}\hat{G}^k_k)(B - E')_{,i}$$
$$\delta\hat{G}^{(\mathrm{gi})\mathrm{i}}_j = \delta\hat{G}^i_j + ({}^{(0)}\hat{G}^i_j)'(B - E'). \tag{2.26}$$

Analogously, for $\delta\hat{T}^{\mu}_{\nu}$ we can choose similar forms. These are obtained according to their transformation forms under gauge. By using the above gauge-invariant variables, we obtain

the gauge-invariant equations for cosmological perturbations,

$$\begin{aligned}
&\Psi'' + \mathcal{H}(\Phi' - \Psi') + \frac{1}{3}\nabla^2(\Phi + 2\Psi) = 8\pi G\varphi'\delta\varphi^{(gi)\prime},\\
&\Psi'' + \mathcal{H}(\Phi' - \Psi') + \nabla^2\Phi - 2(\Phi - \Psi)_{,ii} = 8\pi G\varphi'\delta\varphi^{(gi)\prime},\\
&(\mathcal{H}\Phi + \Psi')_{,i} = 4\pi G\varphi'\delta\varphi^{(gi)}_{,i},\\
&(\Phi - \Psi)_{,ij} = 0,
\end{aligned} \tag{2.27}$$

where $\delta\varphi^{(gi)} = \delta\varphi + \varphi'(B - E')$. It follows from the off-diagonal element that $\Phi = \Psi$. Then the remaining equations are simplified as:

$$\begin{aligned}
&\Phi'' + \nabla^2\Phi = 8\pi G\varphi'\delta\varphi^{(\mathrm{gi})\prime},\\
&\mathcal{H}\Phi + \Phi' = 4\pi G\varphi'\delta\varphi^{(\mathrm{gi})},\\
&\nabla^2 E - 2\Phi - 4\mathcal{H}(B - E') - (B' - E'') = 0,
\end{aligned} \tag{2.28}$$

where the third one is the constraint from the determinant. For the first two equations above, there are no B and E terms involved, and they are essentially the same as two of the equations from GR, which has 3 equations. Although it looks like GR has one more equation, only two of them are actually independent. Consequently, the form of the gauge-invariant perturbations is the same as that in GR. We can see this in more detail by the following. Using the second equation above to express $\delta\varphi^{(gi)}$ in terms of Φ' and Φ, substituting it into the first one, we obtain a second-order partial differential equation for Φ, which can be written as

$$\Phi'' + 2\Big(\mathcal{H} - \frac{\varphi''}{\varphi'}\Big)\Phi' - \nabla^2\Phi + 2\Big(\mathcal{H}' - \mathcal{H}\frac{\varphi''}{\varphi'}\Big)\Phi = 0. \tag{2.29}$$

As in GR, we introduce a gauge-invariant quantity ζ defined by [9, 82]

$$\zeta = \frac{2}{3}\frac{\frac{\dot{\Phi}}{H} + \Phi}{1 + \omega} + \Phi,\ \omega = \frac{p}{\rho}. \tag{2.30}$$

This quantity is conserved for wavelengths far outside the Hubble radius, for which $\nabla^2\Phi$ can be neglected, since

$$\frac{3}{2}\dot{\zeta}H(1+\omega) = \ddot{\Phi} + \Big(H - 2\frac{\ddot{\varphi}}{\dot{\varphi}}\Big)\dot{\Phi} + 2(\dot{H} - H\frac{\ddot{\varphi}}{\dot{\varphi}})\Phi, \tag{2.31}$$

where the right-hand side is the equation (2.29) in terms of physical time neglecting $\nabla^2\Phi$. ζ plays an important role in cosmological perturbations. It will be used to estimate the density perturbation, with which the temperature fluctuation on CMB will be derived.

The equation of motion for the scalar field perturbation $\delta\varphi^{(gi)}$ is derived from the 1st order perturbation of the scalar field equation and is given by

$$\delta\varphi^{(\mathrm{gi})\prime\prime} + 2\mathcal{H}\delta\varphi^{(\mathrm{gi})\prime} - \nabla^2\delta\varphi^{(\mathrm{gi})} + V_{,\varphi\varphi}a^2\delta\varphi^{(\mathrm{gi})} - 4\varphi'\Phi' + 2V_{,\varphi}a^2\Phi = 0. \tag{2.32}$$

In GR, two gauge choices are particularly favored. One is the synchronous gauge, in which $B = 0$ and $\phi = 0$. The other is the longitudinal gauge, in which $B = 0$ and $E = 0$. Due to the extra constraint neither of them is allowed in unimodular relativity. However, we can still apply either $B = 0$ or $B = E'$. This won't change the solution of the second-order partial differential equation for Φ and only affects this relationship between B, E and Φ as in the constraint. If we apply $B = E'$, the constraint will be

$$\nabla^2 E = 2\Phi.$$

If we only apply $B = 0$, we obtain

$$\nabla^2 E + 4\mathcal{H}E' + E'' = 2\Phi.$$

We can see from these equations that Φ is the source of the scalar E. We can also apply $E = 0$, in which case the constraint reduces to

$$2\Phi + 4\mathcal{H}B + B' = 0, \tag{2.33}$$

and from $\Phi = \Psi = \psi - \mathcal{H}B = \phi + \mathcal{H}B + B'$, one obtains

$$\phi = 3\psi. \tag{2.34}$$

For large wavelengths with constant equation of state, Φ is constant. We can rewrite (2.2.3) as

$$(a^4\, B)' = -a^4\Phi. \tag{2.35}$$

In the case of constant Φ and matter-dominated universe, the above equation can be solved as

$$B(x, y, z, \eta) = -\frac{\Phi}{9}\eta + \frac{C}{\eta^8}, \tag{2.36}$$

where C is an integration constant. Since the second term decays quickly, we can approximate $B(x, y, z, \eta)$ with only the first term, making it linear in time as the universe expands. This may have a significant effect on the cosmic microwave background (CMB).

2.3 Cosmological perturbation with hydrodynamical matter

According to the inflation scenario, the universe experienced a period of exponential expansion at early times. After that, the expansion was first dominated by radiation, and a matter-dominated era followed. In this chapter we study the cosmological perturbations with conventional hydrodynamical matter.

2.3.1 FRW background

In the following, we will consider a perfect fluid for which the energy-momentum tensor can be written in terms of only three functions, the energy density ϵ, pressure P and fluid four-velocity u^α,

$$T^\alpha_\beta = (\epsilon + p)u^\alpha u_\beta - p\delta^\alpha_\beta. \tag{2.37}$$

If we choose the background metric to be the FRW metric, there is only one equation of motion in UR 2.5, given by

$$\mathcal{H}^2 - \mathcal{H}' = 4\pi G(\epsilon + p)a^2. \tag{2.38}$$

The conservation of energy gives the second equation,

$$\epsilon' + 3\mathcal{H}(\epsilon + p) = 0. \tag{2.39}$$

If we multiply by $6\mathcal{H}$ on both sides of (2.38) and combine with (2.39), we obtain

$$3\Big(\frac{\mathcal{H}^2}{a^2}\Big)' = 8\pi G\epsilon', \tag{2.40}$$

which can be integrated with an arbitrary integration constant. This constant can be fixed using the current measurement of the acceleration of the universe. At this moment, we will choose the value of this constant to be 0, since it is very small. Then we get a second equation of motion

$$3\mathcal{H}^2 = 8\pi G a^2 \epsilon. \tag{2.41}$$

Again, the trace-free Einstein equation together with the energy conservation equation is equivalent to the Einstein field equation. Therefore, on the FRW background, UG will make the same prediction as GR.

2.3.2 Scalar perturbations

Considering only scalar metric perturbations as in the metric, the perturbed stress-energy tensor has the form

$$\delta T^{\mu}_{\nu} = \begin{pmatrix} \delta\epsilon & -(\epsilon + p)a^{-1}u_i \\ (\epsilon + p)au^i & -\delta p\delta^i_j \end{pmatrix},$$

where $\delta\epsilon$ and δp are the perturbed energy density and pressure, respectively.

As proved in the 1st section, the Einstein field equation can be recovered by the trace-free Einstein field equation combined with the continuity equation. This has been verified by a universe filled by a single scalar field, as well as a perfect fluid on the FRW background. For the perturbation of perfect fluid, we will assume that the continuity equation still holds. Therefore the field equation will be the same as that in GR with one extra constraint due

to the unimodular condition. I will just cite the results from [82],

$$\begin{aligned}\nabla^2\Phi - 3\mathcal{H}\Phi' - 3\mathcal{H}^2\Phi &= 4\pi G a^2 \delta\epsilon^{(gi)},\\ (a\Phi)'_{,i} &= 4\pi G a^2(\epsilon_0 + p_0)\delta u^{(gi)}i,\\ \Phi'' + 3\mathcal{H}\Phi' + (2\mathcal{H}' + \mathcal{H}^2)\Phi &= 4\pi G a^2 \delta p^{(gi)},\end{aligned} \tag{2.42}$$

where $\delta\epsilon^{(gi)} = \delta\epsilon + \epsilon'_0(B - E')$, $\delta p^{(gi)} = \delta p + p'_0(B - E')$ and $\delta u^{(gi)}i = \delta u_i + a(B - E')_{,i}$, and other parameters have the same definition as those in section 2. The constraint due to UR 2.22 is given by

$$\nabla^2 E - 2\Phi - 4\mathcal{H}(B - E') - (B' - E'') = 0. \tag{2.43}$$

Therefore, the gauge-invariant quantity ζ will still be conserved at large wavelengths since it is derived only from the field equations.

2.4 Cosmic Microwave Background Anisotropies

At the beginning of the matter-dominated era, the universe was full of ionized plasma which was strongly coupled with radiation. The temperature was still very high. Thus the mean free path of photons was very short until the time of recombination, at which the protons and electrons combined to form neutral atoms. After that, photons moved freely as the universe expanded. The currently observed CMB are these photons that have escaped since recombination. Since we are looking further and further back in time, we can view the observation of CMB photons as imaging a uniform "surface of last scattering" at a redshift of 1100, which is highly homogeneous and isotropic with temperature $2.72548 \pm 0.00057K$. The anisotropy has been observed at a level of $\frac{\delta T}{T} \backsim 10^{-5}$. Current observation has reached a sensitivity of 10^{-6} [1]. The observational upper bounds of these anisotropies in the CMB provide strong constraints on the spectrum of metric perturbations.

There are three main contributions to the temperature anisotropies of the CMB. First, any peculiar velocity of the observer or the atom emitting photons at recombination gives rise to the Doppler temperature variations. Secondly, the density perturbation for the photons between emission and observation induces temperature fluctuations. Thirdly, the density

perturbation at the time of recombination induces temperature fluctuations too. The simplest contribution to the temperature anisotropy from density fluctuations is a gravitational redshift, known as Sachs-Wolfe effect [90]. The prediction of this effect from GR is given by

$$\frac{\delta T}{T} = \frac{1}{3}\Phi_{\rm em}, \tag{2.44}$$

where $\Phi_{\rm em}$ is the scalar metric perturbation at the time of emission. The purpose of this section is to derive the expression for temperature fluctuations in the framework of UR.

Similarly as in GR, we will apply the approximation of instantaneous recombination in which radiation behaves as an imperfect fluid before recombination, and as an ensemble of free photons immediately afterwards. Therefore, by matching the energy- momentum tensor before and after recombination, we find the relationship between energy density fluctuations and temperature anisotropy.

2.4.1 Before recombination: Baryon-radiation plasma

Before recombination, baryons and radiation are strongly coupled and can be treated as a single imperfect fluid. The energy-momentum tensor is given by [81]

$$T^{\alpha}_{\beta} = (\epsilon + p)u^{\alpha}u_{\beta} - p\,\delta^{\alpha}_{\beta} - \boldsymbol{\eta}\Big(P^{\alpha}_{\gamma}u_{\beta}{}^{;\gamma} + P^{\gamma}_{\beta}u^{\alpha}{}_{;\gamma} - \frac{2}{3}P^{\alpha}_{\beta}u^{\gamma}{}_{;\gamma}\Big), \tag{2.45}$$

where $\boldsymbol{\eta}$ is the shear viscosity coefficient and $P^{\alpha}_{\beta} = \delta^{\alpha}_{\beta} - u^{\alpha}u_{\beta}$ is the spatial projection operator. The energy-momentum tensor is conserved and the 0 component is given by using the perturbed metric at the linear order,

$$\delta\epsilon' + 3\mathcal{H}(\delta\epsilon + \delta p) - 3(\epsilon + p)\psi' + a(\epsilon + p)u^{i}_{,i} - \frac{2\boldsymbol{\eta}\mathcal{H}\nabla^2 B}{a} = 0. \tag{2.46}$$

Note that ϕ does not appear and the shear viscosity appears if we keep $B(x, y, z, t)$ in the metric. For long wavelengths this term can be still neglected, while for short wavelengths it can not be neglected. If we consider long wavelengths, when the baryons are nonrelativistic, this energy conservation law is valid for both baryons and radiation separately. In this case

for the perturbation in the radiation component we obtain

$$(\delta_\gamma - 4\psi)' + \frac{4}{3} a u^i_{,i} = 0, \tag{2.47}$$

where the fractional radiation density perturbation is defined as $\delta_\gamma := \frac{\delta\epsilon_\gamma}{\epsilon_\gamma}$. For the $(0i)$ components of the energy-momentum tensor

$$T^i_0 = a(\epsilon + p)u^i - \frac{\boldsymbol{\eta}\mathcal{H}B_{,i}}{a}, \tag{2.48}$$

where again the shear viscosity appears with $B(x, y, z, t)$. Considering the divergence of this term for long wavelength, we obtain

$$T^i_{0,i} = \frac{4}{3}\epsilon_\gamma u_0 u^i_{,i} = (4\psi - \delta_\gamma)'\epsilon_\gamma, \tag{2.49}$$

where (2.47) has been used.

2.4.2 After recombination: Ensemble of free photons

During the time of recombination, as more and more hydrogen atoms are formed and the temperature drops, photons cease interactions with matter and we consider them as noninteracting identical particles described by kinetic equations. Therefore the distribution function f, characterizing the number density in one-particle phase space, is defined by

$$\mathrm{d}N = f(x^i, p_j, t)\mathrm{d}^3x\mathrm{d}^3p, \tag{2.50}$$

where the position of the particle is given by $x^i(\eta)$ and its 3-momentum is $p_j(\eta)$. For noninteracting particles the distribution function obeys the collisionless Boltzmann equation

$$\frac{Df(x^i(\eta), p_i(\eta), \eta)}{D\eta} \equiv \frac{\partial f}{\partial \eta} + \frac{\mathrm{d}x^i}{\mathrm{d}\eta}\frac{\partial f}{\partial x^i} + \frac{\mathrm{d}p_i}{\mathrm{d}\eta}\frac{\partial f}{\partial p_i} = 0, \tag{2.51}$$

where $\mathrm{d}x^i/\mathrm{d}\eta$ and $\mathrm{d}p_i/\mathrm{d}\eta$ are the derivatives calculated along the geodesics.

For an observer with 4-velocity u^α in an arbitrary coordinate system and a photon with 4-

momentum p_α, the frequency of this photon measured by the observer is given by $\omega = p_\alpha u^\alpha$. If the radiation coming to an observer from different directions

$$l^i \equiv -\frac{p_i}{\Sigma p_i^2} \tag{2.52}$$

has Planckian spectrum, then the distribution function is

$$f = f(\frac{\omega}{T}) \equiv \frac{2}{\exp(\omega/T(x^\alpha, l^i)) - 1}, \tag{2.53}$$

which depends not only on the direction l^i but also on the observer's location x^α and on the moment of time η. In a nearly isotropic universe, the temperature can be written as

$$T(x^\alpha, l^i) = T_0(\eta) + \delta T(x^\alpha, l^i), \tag{2.54}$$

where $\delta T \ll T_0$.

2.4.3 Boltzmann equation

By solving the Boltzmann equation for freely propagating radiation we can find the relationship between the temperature fluctuation and metric perturbations. In GR this is given by $\frac{\delta T}{T} = \frac{1}{3}\Phi$. We expect that Unimodular relativity would predict a modification on this equation. In the folloing we work in the $E = 0$ gauge. Thus the metric perturbations of scalar type involve only ϕ, ψ and B,

$$\mathrm{d}s^2 = a^2(\eta)\left[\,(1+2\phi)\mathrm{d}t^2 - 2B_{,i}\mathrm{d}x^i\mathrm{d}\eta - (1-2\psi)\gamma_{ij}\mathrm{d}x^i\mathrm{d}x^j\,\right]. \tag{2.55}$$

We start with the geodesic equations for radiation in arbitrary curved spacetime,

$$\frac{\mathrm{d}x^\alpha}{\mathrm{d}\lambda} = p^\alpha, \quad \frac{\mathrm{d}p_\alpha}{\mathrm{d}\lambda} = \frac{1}{2}\frac{\partial g_{\gamma\delta}}{\partial x^\alpha}p^\gamma p^\delta, \tag{2.56}$$

where λ is an affine parameter along the geodesic. For photons we have $p^\alpha p_\alpha = 0$ since they have zero mass. Using this relation, up to first order in the metric perturbations, one

obtains

$$\begin{aligned} p^0 &= \frac{(\Sigma p_i^2)^{1/2}}{a^2}(1+\psi-\phi) = \frac{p}{a^2}(1+\psi-\phi), \\ p_0 &= p\,(1+\psi+\phi) - B_{,i}\,p_i. \end{aligned} \tag{2.57}$$

Then from (2.56), we find that

$$\begin{aligned} \frac{\mathrm{d}x^i}{\mathrm{d}\eta} &= \frac{p^i}{p^0} = l^i\,(1+\phi+\psi) + \frac{p_0 B_{,i}}{p}, \\ \frac{\mathrm{d}p_\alpha}{\mathrm{d}\eta} &= \frac{1}{2}\frac{\partial g_{\gamma\delta}}{\partial x^\alpha}\frac{p^\gamma p^\delta}{p^0} = p\,(\psi_{,i}+\phi_{,i}) + p_j\,B_{,ji}, \end{aligned} \tag{2.58}$$

and the Boltzmann equation takes the form

$$\frac{\partial f}{\partial \eta} + \Big[l^i\,(1+\phi+\psi) + \frac{p_0 B_{,i}}{p}\Big]\frac{\partial f}{\partial x^i} + \Big[p\,(\psi_{,i}+\phi_{,i}) + p_j\,B_{,ji}\Big]\frac{\partial f}{\partial p_i} = 0. \tag{2.59}$$

f is a function of the single variable

$$y \equiv \frac{\omega}{T} = \frac{p_0}{T\sqrt{g_{00}}} \backsimeq \frac{1}{T_0 a}[p(1+\psi-\frac{\delta T}{T_0}) - B_{,i}p_i]. \tag{2.60}$$

The Boltzmann equation to zeroth order in the perturbations reduces to

$$(T_0 a)' = 0, \tag{2.61}$$

and to first order becomes

$$(\frac{\partial}{\partial\eta} + l^i\frac{\partial}{\partial x^i})(\phi + \frac{\delta T}{T_0} + l^j B_{,j}) = \frac{\partial}{\partial\eta}(\phi+\psi). \tag{2.62}$$

The zeroth order equation tells us that the temperature is inversely proportional to the scale factor in a homogeneous universe. The linear order determines the temperature fluctuation of the microwave background. After recombination, the universe is matter-dominated. If we write down the right-hand side with the gauge invariant variables, $\phi+\psi = 2\Phi - B'$,

combined with (2.36), then the right-hand side vanishes, while the left-hand side is a total time derivative. Consequently, we obtain

$$(\phi + \frac{\delta T}{T_0} + l^j B_{,j}) = C \tag{2.63}$$

along null geodesics, where C represents a constant. Compared to the traditional Sachs-Wolfe effect, we note that B also contributes to the microwave background fluctuations.

2.4.4 Initial conditions

Consider again the geodesics of photons arriving from direction l^i seen by an observer at the present time η_0 located at x_0^i. Using equation (2.58), one obtains

$$x^i(\eta) \backsimeq x_0^i + l^i(\eta - \eta_0). \tag{2.64}$$

Then the temperature fluctuation $\delta T/T$ in the direction l^i on the sky today is given by

$$\begin{aligned} \frac{\delta T}{T}(\eta_0, x_0^i, l^i) = \quad & \frac{\delta T}{T}(\eta_r, x^i(\eta_r), l^i) + \phi(\eta_r, x^i(\eta_r)) \\ & + l^i B_{,i}(\eta_r, x^i(\eta_r)) - l^i B_{,i}(\eta_0, x_0^i) - \phi(\eta_0, x_0^i), \end{aligned} \tag{2.65}$$

where η_r is the conformal time of recombination and $x^i(\eta_r)$ is given by (2.64). Since we are interested in the l^i dependence of the temperature fluctuation, and the last term only contributes to the monopole component, we will neglect it in the future. Therefore, the angular dependence of $(\delta T/T)_0$ is determined by 3 factors: (1) the initial temperature fluctuations on the last scattering surface; (2) the value of the metric perturbation in the (00) component; (3) the value of the metric perturbation in the $(0i)$ component in the direction of l^i.

For the first contribution, $(\delta T/T)_r$, we can express it in terms of the metric perturbations and the fluctuation of the photon energy density $\delta_\gamma \equiv \delta\epsilon_\gamma/\epsilon_\gamma$ on the last scattering surface. To arrive at this result, we will use matching conditions for the hydrodynamic energy-momentum tensor, which describes the radiation before decoupling, and the kinetic energy-

momentum tensor, which characterizes the gas of free photons after decoupling,

$$T^{\alpha}_{\beta} = \frac{1}{\sqrt{-g}} \int f \frac{p^{\alpha} p_{\beta}}{p^0} \mathrm{d}^3 p. \tag{2.66}$$

Substituting the perturbed metric into the above equation and assuming a Planckian distribution, we get the (00) component of the kinetic energy-momentum tensor

$$\begin{aligned} T^0_0 \quad &\backsimeq \frac{1}{a^4(1+\phi-3\psi)} \int f(\frac{\omega}{T}) p_0 \mathrm{d}^3 p \\ &\backsimeq T_0^4 (1 + 4\frac{\delta T}{T_0} - 2 l^i B_{,i}) \int f(y) y^3 \mathrm{d}y \mathrm{d}^2 l, \end{aligned} \tag{2.67}$$

where $y \equiv \omega/T$. The integration over y can be done straightforwardly and the result combined with $4\pi T_0^4$ represents the energy density of the photon gas after combination. This expression should continuously match the (00) component of the hydrodynamic energy-momentum tensor which characterizes radiation before combination: $T^0_0 = \epsilon_\gamma(1+\delta_\gamma)$. The matching condition implies

$$\delta_\gamma = \int \Big(4\frac{\delta T}{T} - 2 l^i B_{,i}\Big) \frac{\mathrm{d}^2 l}{4\pi}. \tag{2.68}$$

Similarly, one can derive from (2.66) that the other components of the kinetic energy-momentum tensor are:

$$T^i_0 \backsimeq \epsilon_\gamma \int (4 l^i \frac{\delta T}{T} - 2 l^i l^j B_{,j} - B_{,i}) \frac{\mathrm{d}^2 l}{4\pi}. \tag{2.69}$$

Taking the divergence of this term and comparing it to the divergence of the hydrodynamical energy-momentum tensor for radiation before recombination, which is given by (2.49), we get the second matching condition

$$\delta'_\gamma = \int [2 l^i \nabla_i B_{,j} l^j + \nabla_i B_{,i} - 4 l^i \nabla_i (\frac{\delta T}{T})] \frac{\mathrm{d}^2 l}{4\pi}, \tag{2.70}$$

where we have neglected the radiation contribution to the gravitational potential and therefore set $\phi'(\eta_r) = 0$.

To satisfy both (2.68) and (2.70), we find that the spatial Fourier component of the

temperature fluctuations should be related to the energy density inhomogeneities in the radiation and metric perturbations as

$$
\begin{aligned}
&(\frac{\delta T}{T})_{\mathbf{k}}(\mathbf{l},\eta_{\mathbf{r}}) \\
&= \frac{1}{4}\delta_{\mathbf{k}} + \frac{1}{4}\frac{3\,i}{k^2}(k_m l^m)\delta'_{\mathrm{k}} + \frac{1}{2}(l^m k_m)B_{\mathbf{k}}(\mathbf{l},\eta_{\mathbf{r}}),
\end{aligned}
\tag{2.71}
$$

where $\delta_{\mathbf{k}}$ is the Fourier component of δ_γ. Substitute the above equation in the Fourier expansion of (2.65), we obtain the final expression for the temperature fluctuations in the direction $\mathbf{l} \equiv (l^1, l^2, l^3)$ as observed at location $\mathbf{x}_0 \equiv (x^1, x^2, x^3)$:

$$
\begin{aligned}
\frac{\delta T}{T}(\eta_0, \mathbf{x_0}, \mathbf{l}) = \quad & \int \Big[(\phi + \frac{3}{2}(l^m k_m)B + \frac{\delta}{4})_{\mathbf{k}} - \frac{3\,\delta'_{\mathbf{k}}}{4k^2}\frac{\partial}{\partial\eta_0}\Big]_{\eta_r} e^{i\mathbf{k}\cdot(\mathbf{x_0}+\boldsymbol{l}(\eta_{\mathbf{r}}-\eta_{\mathbf{0}}))}\frac{\mathrm{d}^3k}{(2\pi)^{3/2}} \\
& -l^i B_{,i}(\eta_0, x_0^i),
\end{aligned}
\tag{2.72}
$$

where $k \equiv |\mathbf{k}|$, $\mathbf{k}\cdot\mathbf{l} \equiv k_m l^m$ and $\mathbf{k}\cdot\mathbf{x}_0 \equiv k_n x_0^n$. The first term in square brackets represents the combined result from the initial inhomogeneities in the radiation energy density itself and the Sachs-Wolfe effect, the second term is related to the velocities of the baryon-radiation plasma at recombination. The last term shows the effect of present value of B in the perturbed metric. As we can see that for large-scale perturbations, the effect can be neglected. The main source of temperature fluctuations is determined by the energy density perturbation of the radiation.

The density fluctuations of radiation are related to the gravitational potential ψ through Eq.(2.47). We neglect the velocity term in (2.47), which is a good approximation in the long-wavelength regime, and then integrate this equation to arrive at the following relation:

$$
\delta_\gamma - 4\psi = \mathcal{C}\ , \tag{2.73}
$$

where $\mathcal{C}$ is an integration constant to be determined. Consider the universe during the radiation domination epoch. The gravitational potential stays constant on super Hubble scales and hence its value is inherited from the primordial era (such as the one generated

during inflation or an early universe period in one of the alternatives to inflation[1]). If the fluctuations are purely adiabatic, then the first term in the first equation of 2.42 can be neglected, the second term can also be neglected during this era for supper Hubble scales, therefore we arrive at

$$\delta_\gamma^{(\mathrm{gi})} \simeq -2\Phi(\tau \ll \tau_{\mathrm{eq}}) \equiv -2\Phi_{\mathrm{in}} \ , \tag{2.74}$$

where the subscript "in" refers to some moment in the early universe before the time of last scattering. We thus see that the radiation density fluctuation is given by the gravitational potential. If we choose the gauge $E = 0$, then we can use the relation for the gauge variant potential $\Phi = \psi - \mathcal{H}B$, together with $\delta_\gamma^{(\mathrm{gi})} = \delta_\gamma - 4\mathcal{H}B$. Then, we can determine the integration constant $\mathcal{C}$ with the result

$$\mathcal{C} = -6\Phi_{\mathrm{in}} \ . \tag{2.75}$$

Note that if the B term were already important in either the primordial era or the radiation-dominated phase, the above coefficient would obtain an extra contribution, and correspondingly the modification to the SW effect could be even more significant.

After the moment of matter-radiation equality, the cold matter becomes dominant and the equation of state of matter changes. The leads to a change in the value of the gravitational potential Φ on large scales by a factor of 9/10 (this comes from the conservation of ζ, see (2.30)). Afterwards Φ remains constant and so we have,

$$\Phi(\tau \gg \tau_{\mathrm{eq}}) \simeq \frac{9}{10}\Phi_{\mathrm{in}} \ . \tag{2.76}$$

By solving the unimodular constraint equation for B during the period of radiation domination, we find that, when the universe evolves to the recombination, Eq. (2.73) yields

$$\begin{aligned} \delta_\gamma(\tau_{\mathrm{rec}}) &= \mathcal{C} + 4\psi(\tau_{\mathrm{rec}}) \\ &\simeq -\frac{8}{3}\psi(\tau_{\mathrm{rec}}) + 4\mathcal{H}(\tau_{\mathrm{rec}})B(\tau_{\mathrm{rec}}) \ . \end{aligned} \tag{2.77}$$

[1]See e.g. [23] for a recent review of some alternatives to inflation.

Substituting the above expression into Eq.(2.72), and then applying the approximation that $\delta'_{\mathbf{k}} \simeq 0$ on large length scales during the radiation-dominated phase, we obtain the following formula for the resulting temperature fluctuations

$$\frac{\delta T}{T}(\tau_0, \mathbf{x}_0, l^i) \simeq \frac{1}{3}\Phi(\tau_{rec}, \mathbf{x}_0 - \mathbf{l}\tau_0) + \Delta_{\rm UG} \ , \tag{2.78}$$

in terms of the gauge invariant variable Φ. The first term on the right-hand side of the above expression corresponds to the result obtained in GR, which says that the amplitude of temperature fluctuations is given by one third of the gravitational potential on the last scattering surface from which the photons were produced. The second term is the correction term which appears in unimodular gravity and which is a consequence of the non-vanishing quantity B. It takes the form

$$\Delta_{\rm UG} = \int \frac{{\rm d}^3k}{(2\pi)^{3/2}} \Big[- (\frac{3}{4}(\mathbf{k}\cdot\mathbf{l})B_{\mathbf{k}} \Big]_{\tau_{rec}} \times e^{i\mathbf{k}\cdot(\mathbf{x}_0 + \mathbf{l}(\tau_{rec} - \tau_0))} \ . \tag{2.79}$$

We find that the effect of including the shift B on large scales is only dipole like terms. The prediction from unimodular gravity on CMB is then indistinguishable on these scales from that from GR based on current measurements. We have neglected the contribution of radiation to the gravitational potential at recombination and the integrated SW effect, which may lead to important observational signatures.

2.5 Conclusion

In this project, we have studied whether unimodular gravity can be distinguished from GR at the level of cosmological inhomogeneities. We have developed the theory of cosmological perturbations for unimodular gravity, with particular emphasis on the gauge freedom of metric perturbations of scalar type under the group of unimodular coordinate transformations. Our results show that the equation of motion for the gravitational potential is unchanged compared with the result in GR. However, there exists another metric pertur-

bation variable which cannot be set to zero in unimodular gravity, unlike the situation in GR. This is a consequence of the reduced gauge symmetry. On the other hand, the new constraint equation relates this variable to the gravitational potential such that it is not an independent dynamical entity. This variable corresponds to the shift in the perturbed metric, and its value grows in an expanding universe.

We have generalized the Sachs-Wolfe (SW) analysis of the relation between gravitational potential and CMB anisotropies to the case of unimodular gravity. Our results show that the extra metric variable leads both to a modification of the gravitational potential contribution to the CMB anisotropies, and also to a change in the geodesics of light between recombination and the present time. Assuming adiabatic fluctuations, we have shown that on large length scales the relationship between the amplitude of the predicted CMB anisotropies and the amplitude of the gravitational potential differs from the result obtained in GR only by a dipole-like term which is suppressed on large scales. This result was derived under the conservative assumption of neglecting any contribution of the shift during the primordial period before recombination. Since the observational bounds on the difference of the predictions from those obtained in GR are tight, it is worthwhile to revisit our conservative assumptions.

Chapter 3

PROJECT II: CHARGED BLACK HOLES IN DRGT MASSIVE GRAVITY

3.1 dRGT massive gravity

In order to avoid the ghost instability and maintain the Vainshtein mechanism, a family of non-linear ghost-free massive gravity theories was proposed by de Rham, Gabadadze and Tolley (dRGT) in 2010. The corresponding action [38, 40] is given by

$$S = \int d^4x\sqrt{-g}\frac{1}{16\pi G}\Big[R + m^2\mathcal{U}(g,\phi^a)\Big] + S_{\rm matter} \tag{3.1}$$

where R is the Ricci scalar, and $\mathcal{U}$ is a potential for the graviton which modifies the gravitational sector. Specifically, $\mathcal{U}$ is given by

$$\mathcal{U}(g,\phi^a) = \mathcal{U}_2 + \alpha_3\mathcal{U}_3 + \alpha_4\mathcal{U}_4 \ , \tag{3.2}$$

in which α_3 and α_4 are dimensionless parameters. Moreover, by introducing $\mathcal{K}^\mu_\nu = \delta^\mu_\nu - \sqrt{g^{\mu\sigma}\eta_{ab}\partial_\sigma\phi^a\partial_\nu\phi^b}$ and $K^{2\mu}_{\ \ \nu} = K^\mu_\alpha K^\alpha_\nu$, $\mathcal{U}_2$, $\mathcal{U}_3$ and $\mathcal{U}_4$ are defined as

$$\mathcal{U}_2 \equiv [\mathcal{K}]^2 - [\mathcal{K}^2] \ , \tag{3.3}$$

$$\mathcal{U}_3 \equiv [\mathcal{K}]^3 - 3[\mathcal{K}][\mathcal{K}^2] + 2[\mathcal{K}^3] \ , \tag{3.4}$$

$$\mathcal{U}_4 \equiv [\mathcal{K}]^4 - 6[\mathcal{K}]^2[\mathcal{K}^2] + 8[\mathcal{K}][\mathcal{K}^3] + 3[\mathcal{K}^2]^2 - 6[\mathcal{K}^4], \tag{3.5}$$

where the square brackets denote the traces, namely $[\mathcal{K}] = \mathcal{K}^\mu_\mu$. The action is invariant under coordinate transformations $x^\mu \to x^\mu + \epsilon^\mu$ provided π^μ transforms as $\pi^\mu \to \pi^\mu + \epsilon^\mu$.

This action is proved to be ghost-free, at least in the decoupling limit [58, 41]. No higher order terms can be added without introducing the BD ghost [59]. For later convenience, we introduce two new parameters, α and β, as $\alpha_3 = \frac{\alpha-1}{3}$, $\alpha_4 = \frac{\beta}{2} + \frac{1-\alpha}{12}$.

Varying the action with respect to $g_{\mu\nu}$ leads to the modified Einstein equation:

$$G_{\mu\nu} + m^2 X_{\mu\nu} = 8\pi G T_{\mu\nu} \ , \tag{3.6}$$

where $X_{\mu\nu}$ arises from the graviton potential [13]

$$\begin{aligned} X_{\mu\nu} \ = \ & \mathcal{K}_{\mu\nu} - \mathcal{K} g_{\mu\nu} - \alpha \left\{ \mathcal{K}^2_{\mu\nu} - \mathcal{K}\mathcal{K}_{\mu\nu} + \frac{[\mathcal{K}]^2 - [\mathcal{K}^2]}{2} g_{\mu\nu} \right\} \\ & + 6\beta \left\{ \mathcal{K}^3_{\mu\nu} - \mathcal{K}\mathcal{K}^2_{\mu\nu} + \frac{1}{2}\mathcal{K}_{\mu\nu} \left\{ [\mathcal{K}]^2 - [\mathcal{K}^2] \right\} \right\} \\ & - \beta g_{\mu\nu} \left\{ [\mathcal{K}]^3 - 3[\mathcal{K}][\mathcal{K}^2] + 2[\mathcal{K}^3] \right\} \ , \end{aligned} \tag{3.7}$$

and $T_{\mu\nu}$ is the stress-energy momentum obtained from S_{matter}. In addition to the generalized Einstein equation, the Bianchi identity leads to the constraint:

$$\nabla^\mu X_{\mu\nu} = 0 \ . \tag{3.8}$$

3.2 Spherically symmetric solutions

In this project [26], we are interested in the black-hole solutions in the theory of dRGT non-linear massive gravity which carry a static electric charge. We start with the most general form of the static metric respecting spherical symmetry [**?**],

$$ds^2 = -N^2(r)dt^2 + \frac{dr^2}{F^2(r)} + \frac{r^2 d\Omega_2^2}{H^2(r)} \ , \tag{3.9}$$

where $d\Omega_2^2 = d\theta^2 + \sin^2\theta d\varphi^2$.

3.3 Equations of motion

We consider a generic Maxwell field $F_{\mu\nu}$ in curved spacetime, with standard Lagrangian. The Maxwell equations are

$$\partial_\mu(\sqrt{-g}F^{\mu\nu}) = -\sqrt{-g}J^\nu \ , \ \ F_{\mu\nu} = \partial_\mu A_\nu - \partial_\nu A_\mu, \tag{3.10}$$

where J^ν is the current density and A_μ is a vector potential. For a static electric charge Q in the gravitational system, the components of the Maxwell field are:

$$E_r = F_{0r} = E(r) \ , \ \ E_\theta = E_\varphi = 0 \ , \ \ \vec{B} = 0 \ . \tag{3.11}$$

With vanishing source term, the inhomogeneous Maxwell law gives $\partial_r(\sqrt{-g}F^{0r}) = 0$, yielding the solution:

$$E(r) = \frac{QNH^2}{4\pi r^2 F} \ , \tag{3.12}$$

where Q is an integration constant which is typically interpreted as the electric charge, F and H are the metric elements 3.9.

Using the generalized Einstein equation, we find 3 independent equations of motion with 1 constraint from the Bianchi identity. For the "tt" component of the generalized Einstein equation:

$$\begin{aligned}\frac{GQ^2H^6}{4\pi r^2} \quad &= (1+m^2r^2)H^4 + 2m^2r^2(F-3)H^3 - H^2[2r(F\dot{F} - 3m^2r^2) + 3m^2r^2F + F^2] \\ &+2rFH[F(r\ddot{H} + 3\dot{H}) + r\dot{F}\dot{H}] - 5r^2F^2\dot{H}^2 + m^2r^2(H-1)H^2[2H(1-\alpha+3\beta) \\ &-6\beta + F(1-\alpha+6\beta - 3H(1-\alpha+2\beta))] \ . \end{aligned} \tag{3.13}$$

The "rr" component of the generalized Einstein equation takes the form:

$$\begin{aligned}\frac{GQ^2NH^6}{4\pi r^2} &= (1+m^2r^2)NH^4+2m^2r^2(1-3N)H^3+H^2[N(6m^2r^2-F^2)\\ &-r(2F^2\dot{N}+3m^2r^2)]+2rF^2H\dot{H}(r\dot{N}+N)-r^2F^2N\dot{H}^2+m^2r^2(H-1)H^2[1\\ &-\alpha+6\beta(1-N)-H(3(1-\alpha)-2N(1-\alpha+3\beta)+6\beta)]\ . \end{aligned} \tag{3.14}$$

Further, the $\theta\theta$ and $\phi\psi$ components of generalized Einstein equation are essentially the same and is given by

$$\begin{aligned}\frac{GQ^2NH^6}{4\pi r^3} &= m^2rH^3[(3-F)N-1]+2rF^2N\dot{H}^2-FH[rN\dot{F}\dot{H}+F(rN\ddot{H}+r\dot{N}\dot{H}+2N\dot{H})]\\ &+H^2[rF\dot{F}\dot{N}+NF\dot{F}+F^2(r\ddot{N}+\dot{N})+m^2rF(3N-1)-6m^2rN+3m^2r]\\ &+m^2rH^2\{(1-\alpha)[4N-3+H(2-3N)+F(2-3N+H(2N-1))]\\ &+2(F-1)(H-1)(N-1)(2-2\alpha+3\beta)\}\ . \end{aligned} \tag{3.15}$$

In the following we will expand the metric factors around a Minkowski background as [72] $N(r)=1+n(r)$, $F(r)=1+f(r)$, $H(r)=1+h(r)$, and then investigate the linear perturbations. However, we need to be aware of the fact that the factors n and f can be treated as linear perturbations as in General Relativity, while h could, in principle, take large values since this factor corresponds to the strong interactive nature of the scalar mode of graviton. Therefore, we need to keep higher orders in h and truncate the equations of motion to leading order in n and f.

Before expanding the background equations perturbatively, we rescale the radial coordinate by introducing a new metric variable $\rho\equiv\frac{r}{H}$, and correspondingly introduce a new metric factor $1+\tilde{f}=\frac{1+f}{1+h+\rho h'}$, where the prime denotes a derivative with respect to ρ. As a consequence, the linearized metric can be expressed as

$$ds^2=-[1+2n(\rho)]dt^2+[1-2\tilde{f}(\rho)]d\rho^2+\rho^2d\Omega^2, \tag{3.16}$$

which is asymptotic to the Minkowski background when n and $\tilde{f}$ become negligible.

3.4 Solution

3.4.1 Case I: $\alpha = \beta = 0$

First, we consider the case with $\alpha = \beta = 0$. It turns out that all higher order terms of h vanish automatically. We obtain from the linearized equations 3.13 and 3.14

$$n(\rho) \simeq -\frac{4GMe^{-m\rho}}{3\rho} + \frac{GQ^2}{8\pi\rho^2} + \frac{GmQ^2}{16\pi\rho}\left[e^{m\rho}\mathrm{Ei}(-m\rho) - e^{-m\rho}\mathrm{Ei}(m\rho)\right] , \tag{3.17}$$

$$\begin{aligned}\tilde{f}(\rho) \simeq & -\frac{2GMe^{-m\rho}(1+m\rho)}{3\rho} + \frac{GQ^2}{8\pi\rho^2} + \frac{GmQ^2}{32\pi\rho} \times [(1-m\rho)e^{m\rho}\mathrm{Ei}(-m\rho) \\ & - (1+m\rho)e^{-m\rho}\mathrm{Ei}(m\rho)\big] ,\end{aligned} \tag{3.18}$$

where "Ei" is the exponential integral function defined by $\mathrm{Ei}(x) \equiv \int_{-\infty}^{x} e^t \, d\ln t$.

The first post-Newtonian parameter γ is defined as the ratio of $\tilde{f}$ and n: $\gamma \equiv \frac{\tilde{f}}{n}$, in the weak field limit. In the case of General Relativity $\gamma = 1$. For the above solution without electric charge ($Q = 0$), we obtain $\gamma \simeq (1 + m\rho)/2$, and thus in the massless limit it reduces to $\gamma = 1/2$, which is in stark disagreement with the value in General Relativity. This behavior exactly manifests the vDVZ discontinuity. As a consequence, the standard General Relativity result can not be recovered in the spherical system governed by massive gravity with such a parameter choice, and therefore this case is already observationally ruled out.

3.4.2 Case II: $\alpha \neq 0$ and $\beta = 0$

In this case, analytically, we consider two regimes. First in the limit of $\rho \ll \rho_V$, we find that

$$n \simeq \frac{GQ^2}{8\pi\rho^2} - \frac{GM}{\rho} + \frac{m^2\rho_Q^2}{2\alpha^{1/2}}\ln(m\rho) , \tag{3.19}$$

$$\tilde{f} \simeq \frac{GQ^2}{4\pi\rho^2} - \frac{GM}{\rho} - \frac{m^2\rho_Q^2}{\alpha^{1/2}} + \frac{GM\rho}{2\alpha^{1/2}\rho_Q^2} , \tag{3.20}$$

where we have introduced a new parameter for a critical length scale $\rho_Q \equiv \left(\frac{GQ^2}{4\pi m^2}\right)^{1/4}$. When the radial coordinate ρ evolves to the regime which is close to ρ_Q but still smaller than ρ_V, the main contribution of the L.H.S of the equation for h comes from the mass term M. In this case, we only keep the leading order in h, obtaining

$$n \simeq \frac{GQ^2}{8\pi\rho^2} - \frac{GM}{\rho} + \frac{GM\rho}{2\alpha^{2/3}\rho_V^2} , \tag{3.21}$$

$$\tilde{f} \simeq \frac{GQ^2}{8\pi\rho^2} - \frac{GM}{\rho} + \frac{GM}{2\alpha^{1/3}\rho_V} + \frac{GM\rho}{2\alpha^{2/3}\rho_V^2} . \tag{3.22}$$

We also numerically evolve the perturbation equation.

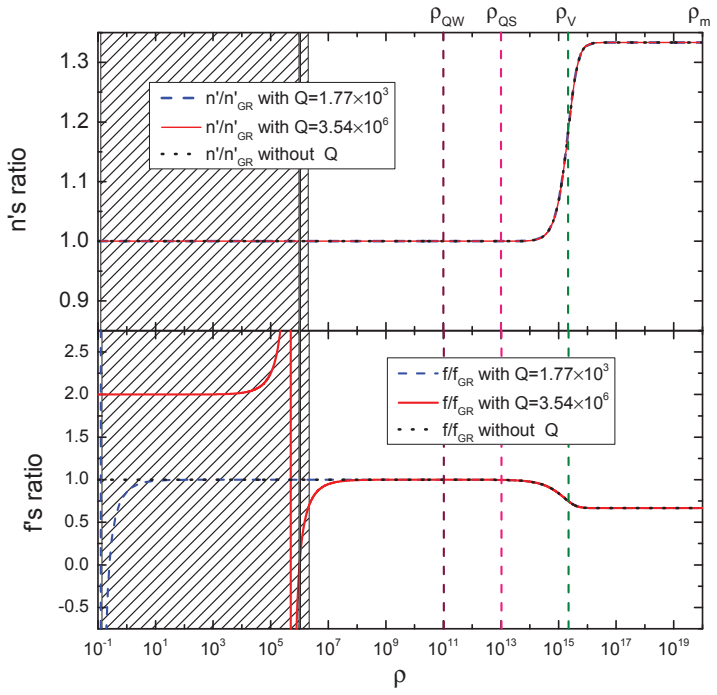

Figure 3.1. *Plot of the evolutions of the ratios n'/n'_{GR} and $\tilde{f}/\tilde{f}_{GR}$ as functions of the radial coordinate ρ in a charged spherical system described by nonlinear massive gravity. The model parameters are taken as: $\alpha = 1$ and $\beta = 0$. In the numerical calculation, we take $m = 10^{-20}$ and $M = 10^6$. The corresponding Compton wavelength $\rho_m = 10^{20}$ and the Vainshtein radius $\rho_V = 2.15 \times 10^{15}$ are denoted on the top of the figure. The values of weak and strong electric charges are provided in the plot. All dimensional parameters are in Planck units. The "f" in the lower panel represents for the metric factor $\tilde{f}$ in the main text.*

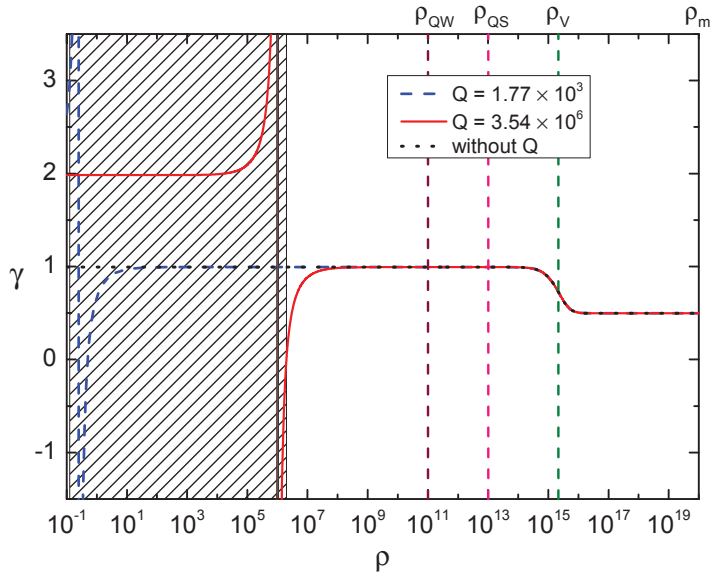

Figure 3.2. *Plot of the evolutions of the post-Newtonian parameter γ as functions of the radial coordinate ρ in a charged spherical system described by nonlinear massive gravity. In the numerical calculation, the parameters are chosen to be the same as those provided in Fig. 3.1*

3.4.3 Case III: $\beta \neq 0$

The case where both α,β parameters are non vanishing can be divided in two subcases: $\beta < 0$ and $\beta > 0$.

$\beta < 0$

As shown in this figure $h \ll 1$ in the range $r_S < \rho < \rho_Q$. Thus, in the semi-analytical calculation, we keep the leading order terms of the equations of motion for the metric factors, and then we obtain

$$n' \simeq -\frac{m^2}{2\beta^{1/3}}\left(\frac{{\rho_Q}^4}{\rho} - {\rho_V}^3\right)^{1/3}, \tag{3.23}$$

$$\tilde{f} \simeq -\frac{GQ^2}{8\pi\rho^2} + \frac{\alpha m^2}{2\beta^{2/3}}\left(\frac{{\rho_Q}^4}{\rho} - {\rho_V}^3\right)^{2/3} - \frac{m^2}{2\beta^{1/3}}\left({\rho_Q}^4 - \rho{\rho_V}^3\right)^{1/3}\rho^{2/3}. \tag{3.24}$$

From the above semi-analytic results we find that the corrections to $\tilde{f}$ and n are so dramatic that the usual Schwarzschild-like gravitational potential (in the form $1/\rho$) is exactly

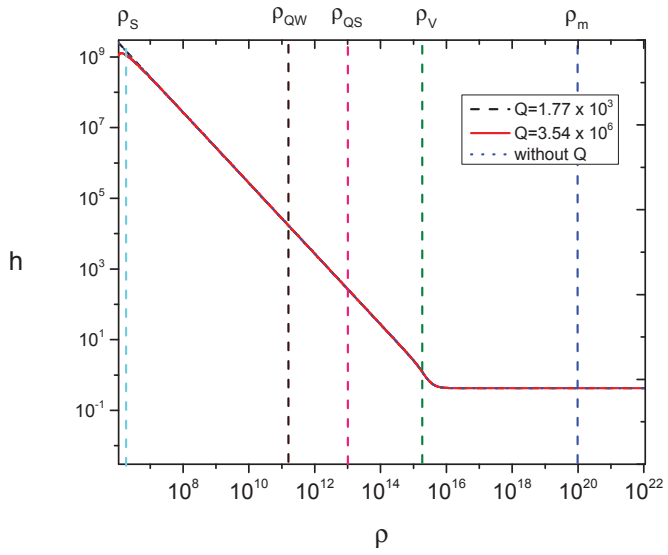

Figure 3.3. *Plot of the evolution of the metric factor h as a function of the radial coordinate ρ in a charged spherical system described by nonlinear massive gravity. The parameters of the massive gravity model are taken as: $\alpha = 1$ and $\beta = -1/2$. Moreover, m and M are the same as those provided in Fig 3.1.*

canceled. This result agrees with the conclusion of [72] in which a neutral spherical system was considered.

$\beta > 0$

Apart from the previous solution in which h is large-valued below the Vainshtein radius, there exists a second solution in which the metric factor h always takes a small value outside the Schwarzschild radius.

For this case, in a strongly charged spherical system the absolute value $|h|$ can become larger than 1 inside the Schwarzschild radius. As we move away from the Schwarzschild radius h evolves to a constant, which coincides with the value when the charge is weak. After crossing the Vainshtein radius h approaches 0 rapidly. By comparing $\tilde{f}$ and n' with the results of General Relativity, we can clearly see the Vainshtein mechanism from Fig. 3.4.

$\beta = \alpha^2/6$*: An exact analytic solution*

We insert the relation $\beta = \alpha^2/6$ into the nonlinear equation of motion of f and we find that there exists a special solution for h, namely $h = \frac{1}{\alpha}$, which implies a constant metric factor $H = (1+\alpha)/\alpha$. Working with the r coordinate directly, by performing the coordinate

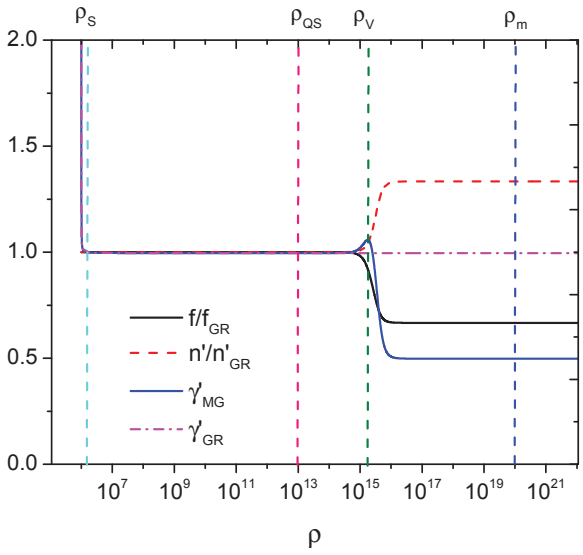

Figure 3.4. *Plot of the evolutions of the ratios n'/n'_{GR}, $\tilde{f}/\tilde{f}_{GR}$, and the quotient $\gamma \equiv \frac{\tilde{f}'}{n'}$ as functions of the radial coordinate ρ in a charged spherical system described by nonlinear massive gravity. The parameters of the massive gravity model are taken as: $\alpha = 1$, $\beta = 3$. Other parameters are the same as those used in Fig. 3.3. The 'f' in the plot represents the metric factor $\tilde{f}$ in the main text.*

rescaling $t \to \frac{\alpha}{1+\alpha}t$, $r \to \frac{1+\alpha}{\alpha}r$, and introducing two coefficients $\tilde{r}_S \equiv \frac{\alpha^3 r_M}{(1+\alpha)^3}$, $r_\Lambda \equiv \frac{\sqrt{3\alpha}}{m}$, which are related to the Schwarzschild radius and the de Sitter radius, respectively, we get the exact form of the RN-dS-like solution as

$$ds^2 = -A(r)dt^2 + \frac{dr^2}{A(r)} + r^2 d\Omega^2 \ , \tag{3.25}$$

with $A(r) = 1 + \frac{r_Q^2}{r^2} - \frac{\tilde{r}_S}{r} - \frac{r^2}{r_\Lambda^2}$. The above solution can recover the standard RN result in General Relativity, and $\tilde{r}_S$ coincides to the usual Schwarzschild radius r_S when we take $m = 0$. Furthermore, our result is in agreement with the one obtained in [85]; however we did not introduce an additional cosmological constant in order to see whether and how a pure massive gravity model can yield a dS background by itself.

3.5 Conclusion

In conclusion, by investigating the spherically symmetric charged system in the context of dRGT non-linear massive gravity we can analyse the parameter space of this model. We

find that depending on the different dynamics of our solutions, the solution parameter space can be roughly categorized into three parts:

- The first class corresponds to $\alpha = \beta = 0$ and thus the graviton's potential takes a fixed form. The solution in this subclass is well described at the perturbative level, but the vDVZ discontinuity cannot be avoided. However, the post-Newtonian parameter in this class fails to agree with General Relativity and thus the corresponding parameter choice is observationally ruled out.

- In the second subclass, we keep $\beta = 0$ but we allow α to be an arbitrary constant. The corresponding solution shows that General Relativity can be recovered between the outer horizon of the black hole and the Vainshtein radius by virtue of the Vainshtein mechanism. This scenario is similar to the case of the neutral black hole in massive gravity. However, the existence of an electric charge could increase the value of the metric factor h within a newly defined radius ρ_Q and thus the detailed evolutions of time-like and space-like metric components behave differently from those of a neutral black hole. Namely, the metric factor n obtains a logarithmic correction when the radius is close to the outer horizon.

- The third subclass of parameter choice is the most general in the parameter space, which requires both α and β to be non-vanishing. In this case the solutions behave dramatically differently depending on the positivity of β. When $\beta < 0$ the strongly coupled scalar graviton greatly decreases the strength of gravity at small length scales, and thus the usual Schwarzschild-like gravitational potential totally disappears which severely challenges all astronomical observations. However, if β is positive General Relativity can be recovered again through the Vainshtein mechanism. This behavior is similar to the solution in the second subclass with $\beta = 0$. Therefore, the solution in this case, together with the solution in the second subclass, might provide a certain parameter space for nonlinear massive gravity to conform with current solar system observations.

- Finally, there exists a particular parameter choice in the last subclass which suggests $\beta = \alpha^2/6$. Under this condition the background equations of motion can be solved exactly and yield a solution which is identical to the RN-dS form in which only the dS radius r_Λ contains the model parameter α. The exact solution with such a special parameter choice can recover the standard result in General Relativity in the limit of either a vanishing graviton mass or an extremely large value of the parameter α.

Chapter 4

PROJECT III: CONSTRAINTS ON THE GRAVITON MASS FROM THE COSMIC MICROWAVE BACKGROUND RADIATION

4.1 Introduction

Among current massive gravity theories [3, 37, 59], there is one class which is phenomenologically closely related to GR [11, 27, 28, 37, 43, 44, 45, 56, 60, 101]. They share the same background equations of motion with GR, as well as the evolution for scalar and vector fluctuations. Only tensor fluctuations are modified with the graviton mass, which is time dependent in general [56]. In other words, the dispersion relation for gravitational waves is given by $\omega^2 = k^2 + {m_g}^2$. For the sake of simplicity, we will only focus on these theories in this project. Based on this modification to GR, by checking Kepler's third law for planets in the solar system, the constraint on the graviton mass is found to be $m_g \lesssim 2.2 \times 10^{-22}\,\mathrm{eV}$ [4, 25]. By comparing electromagnetic wave observations and gravitational wave observations from future space-based detectors Laser Interferometer Space Antenna (LISA), the bound on graviton mass could be $m_g \lesssim 10^{-26}\mathrm{eV}$ [35, 68]. By studying gravitational waves from inspiralling compact binaries, in which a varying speed for different wavelengths leads to a shorter time difference between emission time and arrival time compared to the massless case in which the speed of gravitational waves is constant, the ground-based Laser Interferometer Gravitational-Wave Observatory (LIGO) and space-based LISA would bound the graviton mass to be $m_g \lesssim 1\times10^{-22}\,\mathrm{eV}$ and $m_g \lesssim 1\times10^{-26}\,\mathrm{eV}$ respectively [14, 15, 51, 73, 98, 99, 108]. More stringent bounds can be found from galactic and cluster dynamics as $m_g \lesssim 1\times10^{-29}\,\mathrm{eV}$

[19] and weak lensing as $m_g \lesssim 6.9 \times 10^{-32}$ eV [30]. By studying the stability of Schwarzschild and Kerr black holes under linear tensor perturbations, a bound on the graviton mass is found to be $m_g \lesssim 5 \times 10^{-23}$eV [24].

Another way to constrain the value of the graviton mass is to study the B-mode polarization pattern on the CMB [10, 34, 54, 65, 67, 93]. Scalar perturbations only contribute to E modes. Both tensor and vector perturbations could generate the B modes. However, the vector perturbations were damped quickly by the expansion of the universe [66]. Therefore, the B modes polarization plays an important role in searching for gravitational waves and any detection of them will place significant constraints on cosmological models and also on the mass of the graviton [17, 42]. There are also secondary sources of B modes such as gravitational lensing [57, 112], and galactic synchrotron emission [52]. In this project we will only focus on the signature of massive primordial gravitational waves on the B mode polarization in contrast to the massless case. In the following sections we will first give a brief review of the CMB polarization and then proceed to the tensor contribution. In the last part we will show the polarization pattern for massive gravitons in comparison with the massless case.

4.2 Microwave Background polarization

4.2.1 Stokes parameters

Polarized light is conventionally described by Stokes parameters proposed by G.G. Stokes in 1852. They are quadratic in the field strength and can be determined through intensity measurements together with a linear polarizer and a quarter-wave plate or equivalents in the lab. One important property is that they are additive for incoherent superpositions of waves. Consider a nearly monochromatic plane electromagnetic wave with mean frequency ω propagating in the z direction. Its electric field vector in space can be decomposed as

$$E_x = a_x(t)\cos[\omega t - \theta_x(t)], \quad E_y = a_y(t)\cos[\omega t - \theta_y(t)]. \tag{4.1}$$

The Stokes parameters are defined as [62]

$$\begin{aligned} I \equiv &\quad \langle a_x^2 \rangle + \langle a_y^2 \rangle, \\ Q \equiv &\quad \langle a_x^2 \rangle - \langle a_y^2 \rangle, \\ U \equiv &\quad \langle 2a_x a_y \cos(\theta_x - \theta_y) \rangle, \\ V \equiv &\quad \langle 2a_x a_y \sin(\theta_x - \theta_y) \rangle, \end{aligned} \tag{4.2}$$

where the angle brackets represent time average. The parameter I measures the intensity of the wave and is proportional to the temperature. The other three parameters define the polarization state of the wave. Unpolarized light is described by $Q = U = V = 0$. For linear polarization the phase angles satisfy $\theta_x = \theta_y$. The parameter V describes circular polarization and it can be ignored in cosmology since it can not be generated through Thomson scattering [70].

Since CMB radiation come to us from all directions and it is like coming from a spherical surface, which is the last scattering surface, it is convenient to use spherical coordinates. In the following we will use the unit vector $\hat{\mathbf{n}}$ to denote the direction of light coming to the observer, and the other two orthogonal vectors are $\hat{\mathbf{e}}_\theta$ and $\hat{\mathbf{e}}_\phi$. The intensity parameter I is invariant under a rotation in the plane perpendicular to $\hat{\mathbf{n}}$, while Q and U depend on the orientation of the $\hat{\mathbf{e}}_\theta$ and $\hat{\mathbf{e}}_\phi$ axes. Under a rotation on the plane by an angle ψ, Q and U transform as

$$\begin{aligned} Q'(\hat{\mathbf{n}}) = &\quad Q\cos 2\psi + U \sin 2\psi, \\ U'(\hat{\mathbf{n}}) = &\quad -Q\sin 2\psi + U\cos 2\psi, \end{aligned} \tag{4.3}$$

where $\hat{\mathbf{e}}'_\theta = \cos\phi\,\hat{\mathbf{e}}_\theta + \sin\phi\,\hat{\mathbf{e}}_\phi$ and $\hat{\mathbf{e}}'_\phi = -\sin\phi\,\hat{\mathbf{e}}_\theta + \cos\phi\,\hat{\mathbf{e}}_\phi$. It is convenient to construct two quantities which have a definite value of spin and transform under the above rotation,

$$(Q \pm iU)'(\hat{\mathbf{n}}) = e^{\mp 2i\psi}(Q \pm iU). \tag{4.4}$$

According to the definition of spin-weighted functions [100, 111], the temperature, which is

related to the intensity by $I = \sigma T^4$, has spin 0, while the two complex quantities constructed above have spin-weights 2 and -2 respectively. Spin s spherical harmonics form a complete and orthonormal basis. Hence, we can decompose the above quantities into these spin-weighted spherical harmonics,

$$\begin{aligned} T(\hat{\mathbf{n}}) = & \quad \sum_{lm} a_{T,lm} \mathrm{Y_{lm}}(\hat{\mathbf{n}}), \\ (Q+iU)(\hat{\mathbf{n}}) = & \quad \sum_{lm} a_{2,lm}\ {}_2\mathrm{Y_{lm}}(\hat{\mathbf{n}}), \\ (Q-iU)(\hat{\mathbf{n}}) = & \quad \sum_{lm} a_{-2,lm}\ {}_{-2}\mathrm{Y_{lm}}(\hat{\mathbf{n}}). \end{aligned} \tag{4.5}$$

To calculate Q and U, there exists one coordinate system in which Q and U can be easily calculated where the wave vector $\mathbf{k}$ is parallel to $\hat{\mathrm{z}}$. The superposition of different modes makes the calculation complicated, due to the transformation behavior of Q and U under rotation. Therefore it is convenient to work with coordinate invariant quantities like the temperature. One benefit of spin-weighted harmonics is that there exist spin raising and lowering operators $\eth$ and $\bar{\eth}$ which can act on the spin s quantities to get a spin 0 one, which is invariant under coordinate transformations. A brief review about spin s spherical harmonics is given in Appendix 3. By acting twice with a spin lowering and raising operator on $Q+iU$ and $Q-iU$, respectively, one obtains

$$\begin{aligned} \bar{\eth}^2(Q+iU)'(\hat{\mathbf{n}}) &= \sum_{lm} \big[\frac{(l+2)!}{(l-2)!}\big]^{1/2} a_{2,lm}\, Y_{lm}(\hat{\mathbf{n}}), \\ \eth^2(Q-iU)'(\hat{\mathbf{n}}) &= \sum_{lm} \big[\frac{(l+2)!}{(l-2)!}\big]^{1/2} a_{-2,lm}\, Y_{lm}(\hat{\mathbf{n}}). \end{aligned} \tag{4.6}$$

The above two quantities are rotationally invariant just like temperature, therefore together

with equations 4.5, we can write the expansion coefficients of the spherical harmonics as

$$\begin{aligned}
a_{T,lm} &= \int d\Omega\, Y^*_{lm}(\hat{\mathbf{n}})\, T(\hat{\mathbf{n}}), \\
a_{2,lm} &= \int d\Omega\ {}_2Y^*_{lm}(\hat{\mathbf{n}})(Q+iU)(\hat{\mathbf{n}}) \\
&= \big[\frac{(l+2)!}{(l-2)!}\big]^{-1/2} \int d\Omega\ Y^*_{lm}(\hat{\mathbf{n}})\ \bar{\eth}^2(Q+iU)(\hat{\mathbf{n}}), \\
a_{-2,lm} &= \int d\Omega\ {}_{-2}Y^*_{lm}(\hat{\mathbf{n}})(Q-iU)(\hat{\mathbf{n}}) \\
&= \big[\frac{(l+2)!}{(l-2)!}\big]^{-1/2} \int d\Omega\ Y^*_{lm}(\hat{\mathbf{n}})\ \eth^2(Q-iU)(\hat{\mathbf{n}}).
\end{aligned} \tag{4.7}$$

The E modes and B modes are two independent linear combinations of $a_{2,lm}$ and $a_{-2,lm}$,

$$\begin{aligned}
a_{E,lm} &= -(a_{2,lm} + a_{-2,lm})/2 \\
a_{B,lm} &= i(a_{2,lm} - a_{-2,lm})/2
\end{aligned} \tag{4.8}$$

It is more convenient to work with them in cosmology. They have different parity transformation properties. Under $\hat{\mathbf{n}} \to -\hat{\mathbf{n}}$, E modes remain the same while B modes change sign in analogy with electric and magnetic fields. It is also useful to introduce two scalar quantities $\tilde{E}(\hat{\mathbf{n}})$ and $\tilde{B}(\hat{\mathbf{n}})$ [111]

$$\begin{aligned}
\tilde{E}(\hat{\mathbf{n}}) &\equiv -\frac{1}{2}\big[\bar{\eth}^2(Q+iU) + \eth^2(Q-iU)\big] \\
&\equiv \sum_{lm} \big[\frac{(l+2)!}{(l-2)!}\big]^{1/2} a_{E,lm}\, Y_{lm}(\hat{\mathbf{n}}), \\
\tilde{B}(\hat{\mathbf{n}}) &\equiv \frac{i}{2}\big[\bar{\eth}^2(Q+iU) - \eth^2(Q-iU)\big] \\
&\equiv \sum_{lm} \big[\frac{(l+2)!}{(l-2)!}\big]^{1/2} a_{B,lm}\, Y_{lm}(\hat{\mathbf{n}}).
\end{aligned} \tag{4.9}$$

They are rotationally invariant and are useful for calculations in real space as we will see in the following.

A sky map of the CMB temperature and polarization fluctuations can be fully characterized in terms of an infinite sequence of correlation functions. If the spectrum of fluctuations

is Gaussian, as predicted by inflation and as current data suggests, then only the even order correlation functions are nonzero and all of them can be expressed through the two-point correlation function. In this project we will just focus on the two point correlation function,

$$\begin{aligned} C^{TT}(\theta) &\equiv \big\langle \delta T(\mathbf{n}_1)\delta T(\mathbf{n}_2)\big\rangle \\ C^{EE}(\theta) &\equiv \big\langle E(\mathbf{n}_1)\, E(\mathbf{n}_2)\big\rangle \\ C^{BB}(\theta) &\equiv \big\langle B(\mathbf{n}_1)\, B(\mathbf{n}_2)\big\rangle \\ C^{ET}(\theta) &\equiv \big\langle E(\mathbf{n}_1)\, \delta T(\mathbf{n}_2)\big\rangle, \end{aligned} \tag{4.10}$$

where the arrow brackets denote averaging over all directions $\mathbf{n_1}$ and $\mathbf{n_2}$ satisfying the condition $\mathbf{n}_1 \cdot \mathbf{n}_2 = \cos(\theta)$. The cross correlation between B and E or B and T vanishes because B has opposite parity of T and E. We can write functions of θ as expansions of the legendre polynomials, which is complete and orthogonal,

$$C(\theta) = \frac{1}{4\pi}\sum_{i=2}^{\infty}(2l+1)\, C_l\, P_l(\cos(\theta)). \tag{4.11}$$

The power spectra in the Fourier space, or the multipole moments, C_l^{TT}, C_l^{EE}, C_l^{BB} and C_l^{TE} can then be found from the above expansion. Equivalently they can also be calculated according to equations 4.5, 4.9,

$$\begin{aligned} C_l^{TT} &= \frac{1}{2l+1}\sum_m \big\langle a^*_{T,lm} a_{T,lm}\big\rangle \\ C_l^{EE} &= \frac{1}{2l+1}\sum_m \big\langle a^*_{E,lm} a_{E,lm}\big\rangle \\ C_l^{BB} &= \frac{1}{2l+1}\sum_m \big\langle a^*_{B,lm} a_{B,lm}\big\rangle \\ C_l^{TE} &= \frac{1}{2l+1}\sum_m \big\langle a^*_{T,lm} a_{E,lm}\big\rangle, \end{aligned} \tag{4.12}$$

where the brackets refer to a cosmic mean, average of the results obtained by observers in all space for a given l. Since our universe is homogeneous and isotropic on large scales, the

average over all directions as in equation 4.10 on the sky from one observation point (as us the earth) should be close to the cosmic mean.

4.2.2 Thomson scattering

The radiation of CMB is expected to be polarized because of Compton scattering [61, 70, 101]. Before recombination, due to the intense random motion of photons and baryons, any polarization would disappear instantly as it was created. After recombination, photons propagate freely along geodesics and any polarization produced at recombination will remain fixed. Therefore if we can observe the polarization on CMB today, it will contain information about the last scattering surface, complementary to the temperature anisotropies. In this section we will focus on how the polarization is generated in CMB from Thomson scattering.

Light traveling in the z direction has electric and magnetic fields oscillating in the $x-y$ plane. If the intensity on the two transverse directions is equal, then the light is unpolarized, otherwise it would be polarized. Thomson scattering can generate polarization since it allows transverse radiation to go through and stops any radiation parallel to the outgoing direction as shown in the figure 4.1, in which the unpolarized light coming from the x axis is scattered off the electron to the z axis and the outgoing light is polarized along the y axis. If the

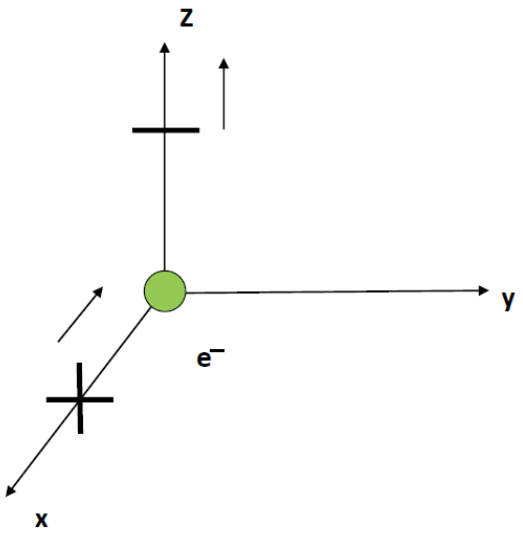

Figure 4.1. *Unpolarized light coming from the x axis toward the origin is scattered by an electron at the center into the $+z$ direction.*

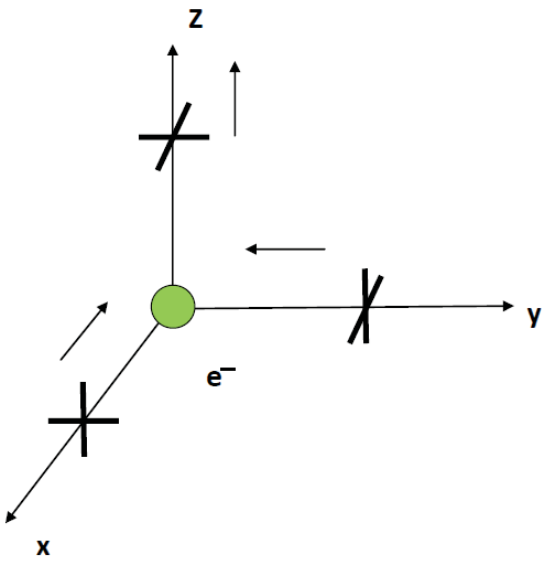

Figure 4.2. *Two unpolarized light rays coming from the x axis and y axis with the same intensity toward the origin are both scattered by an electron at the center into the $+z$ direction.*

incident radiation is isotropic, then polarization can not be generated. As shown in figure 4.2, if there is unpolarized light coming from both the x and y axis with the same intensity, the outgoing light along the z axis will have equal intensity along x and y direction, hence unpolarized.

Instead of isotropic incoming radiation, quadrupole anisotropic distribution induces polarization after Thomson scattering, as shown in figure 4.3.

In fact to produce polarized radiation, the incoming radiation must have a nonzero quadrupole [70]. As shown in Figure 4.4, unpolarized incoming light with intensity I' along direction $\hat{\mathbf{n}}'$ is scattered into direction $\hat{\mathbf{n}}$, which is described by Stokes parameters I, Q, U and V. Two axes perpendicular to the incoming photon are $\hat{\epsilon}'_1$ and $\hat{\epsilon}'_2$ with the latter one in the scattering surface. Polarization vectors for the outgoing light are $\hat{\epsilon}_1$ and $\hat{\epsilon}_2$ with the latter one in the scattering surface. The Thomson scattering cross section for incident radiation with linear polarization vector ϵ' being scattered into a wave with linear polarization vector ϵ is given by

$$\frac{d\sigma}{d\Omega} = \frac{3\sigma_T}{8\pi}|\epsilon' \cdot \epsilon|, \tag{4.13}$$

where σ_T is the total Thomson scattering cross section. To take the dot products, it is useful

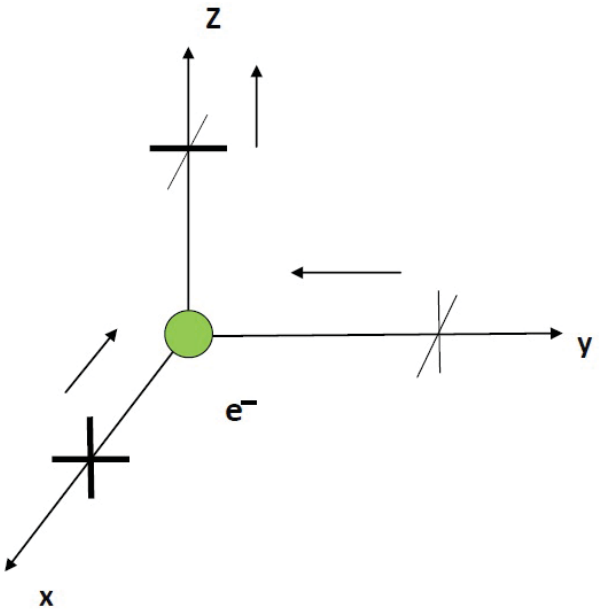

Figure 4.3. *Incoming radiation produces polarization. The intensity of light coming from the x axis is stronger than that from the y axis.*

to consider $\hat{\mathbf{n}} = \hat{\mathbf{z}}$, $\hat{\epsilon}_1 = \hat{\mathbf{x}}$ and $\hat{\epsilon}_2 = \hat{\mathbf{y}}$. Then express $\hat{\mathbf{n}}'$ and $\hat{\epsilon}'$ in terms of their Cartesian coordinates. We have

$$\begin{aligned} \hat{\mathbf{n}}' &= (\sin\theta'\cos\phi', \sin\theta'\sin\phi', \cos\theta) \\ \hat{\epsilon}'_1 &= (\cos\theta'\cos\phi', \cos\theta'\sin\phi', -\sin\theta') \\ \hat{\epsilon}'_2 &= (-\sin\phi', \cos\phi', 0). \end{aligned} \tag{4.14}$$

By integrating all incoming radiation intensities, we obtain

$$\begin{aligned} I(\hat{\mathbf{z}}) &= \frac{3\sigma_T}{16\pi}\int d\Omega\,(1+\cos\theta'^2)\,I'(\theta',\phi') \\ Q(\hat{\mathbf{z}}) &= \frac{3\sigma_T}{16\pi}\int d\Omega\,\sin\theta'^2\cos(2\phi')\,I'(\theta',\phi') \\ U(\hat{\mathbf{z}}) &= \frac{3\sigma_T}{16\pi}\int d\Omega\,\sin\theta'^2\sin(2\phi')\,I'(\theta',\phi'), \end{aligned} \tag{4.15}$$

where θ' and ϕ' are the spherical coordinates for the incoming radiation $\hat{\mathbf{n}}'$ in contrast with the spherical coordinates θ and ϕ for the outgoing radiation $\hat{\mathbf{n}}$ with respect to observers (us)

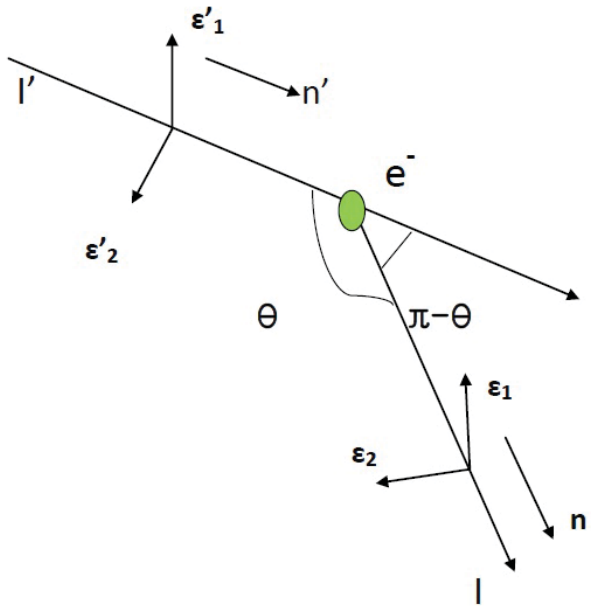

Figure 4.4. *Thomson scattering: incident light with intensity I' is scattered by the electron at the origin into the light with intensity I. The angle between the incident ray and the outgoing ray is θ. ϵ' are the incoming polarization vectors, while ϵ are the outgoing polarization vectors.*

at the center. For Q and U, the combination of angles in the integrand is proportional to the sum of the spherical harmonics $Y_{2,2}+Y_{2,-2}$ and $Y_{2,2}-Y_{2,-2}$ respectively. We can also see that the outgoing polarization state depends only on the intensity distribution of the unpolarized incident radiation. Since the spherical harmonics are orthogonal, the integral will only pick up $l = 2$, $m = \pm 2$ components of the incident intensity. Nonzero polarization can be created only if the incident radiation has a quadrupole component. This is in agreement with figure 4.2.

4.3 The Boltzmann equation for tensor perturbations

To get the current power spectra of the CMB from equation 4.12 using the equation 4.7, we need to study the propagation of photons following geodesics from the last scattering surface in the perturbed FRW spacetime. As the calculation is based on linear perturbation theory, in which case different modes evolve independently in the Fourier space and we are interested in the signature of the graviton mass on the spectra, we will only study the tensor perturbations of the metric. We will solve part of the Boltzmann equation with Thomson

collision term in a flat universe with metric

$$
\begin{aligned}
&g_{00} = 1, \;\; g_{0i} = 0 \\
&g_{ij} = -a(t)^2\big[\delta_{ij} + h_{ij}(\mathbf{x}, t)\big],
\end{aligned} \tag{4.16}
$$

where the tensor metric is transverse-traceless $h^i_i = 0$, $\partial^j h_{ij} = 0$ in which case only pure tensor modes are considered. The inverse metric to first order is given by

$$
\begin{aligned}
&g^{00} = 1, \;\; g^{oi} = 0 \\
&g^{ij} = -\frac{1}{a(t)^2}\big[\delta^{ij} - h^{ij}(\mathbf{x}, t)\big].
\end{aligned} \tag{4.17}
$$

Photons are described by space-time coordinates x^μ and four-momentum p^μ. Their geodesic equations can be written as

$$
\begin{aligned}
&\frac{d^2x^\mu}{d\lambda^2} + \Gamma^\mu_{\alpha\beta}\frac{dx^\alpha}{dx^\beta} = 0 \\
&\frac{dx^\mu}{d\lambda} = p^\mu \\
&g_{\alpha\beta}\frac{dx^\alpha}{d\lambda}\frac{dx^\beta}{d\lambda} = 0,
\end{aligned} \tag{4.18}
$$

where λ is an affine parameter along the geodesics. Then we obtain that

$$
\begin{aligned}
&\frac{\mathbf{p}^i}{p^0} = \frac{dx^i}{dt} \\
&\mathbf{p}^i = \frac{1}{a}p\hat{p}^i(1 - \frac{1}{2}\hat{\mathbf{p}}^m\hat{\mathbf{p}}^n h_{mn}),
\end{aligned} \tag{4.19}
$$

where $p = (-\mathbf{p}^i\mathbf{p}_i)^{1/2}$ and $\hat{\mathbf{p}}$ is the unit vector. Combined with the geodesic equation we find that

$$
\frac{dp}{dt} = -p\big[\frac{\dot{a}}{a} + \frac{1}{2}\hat{\mathbf{p}}^i\hat{\mathbf{p}}^j\frac{\partial h_{ij}}{\partial t}\big]. \tag{4.20}
$$

The Boltzmann equation for any phase-space distribution function f is [70]

$$\frac{df}{dt} = \frac{\partial f}{\partial t} + \frac{\partial f}{\partial x^i}\frac{\mathbf{p}^i}{p^0} + \frac{\partial f}{\partial p}\frac{dp}{dt} + \frac{\partial f}{\partial \hat{\mathbf{p}}^i}\frac{d\hat{\mathbf{p}}^i}{dt} = C(\mathbf{x}, p^\mu), \tag{4.21}$$

where the collision term $C(\mathbf{x}, p^\mu)$ is given by quantum electrodynamics. Since we are considering linear perturbation theory, we expand the distribution function as

$$f(\mathbf{x}, p, \hat{\mathbf{p}}, t) = f^0(p, t) + f^1(\mathbf{x}, p, \hat{\mathbf{p}}, t). \tag{4.22}$$

At the zeroth order, the collision term can be neglected and the solution gives $f^0(p,t) = f^0(pa)$ which proves that wavelengths are redshifted with cosmological expansion. The first order equation after Fourier transformation over the spatial dependence is given by

$$\frac{\partial}{\partial t}f^1(\mathbf{k}, p, \hat{\mathbf{p}}) + \frac{i}{a}(\mathbf{k}\cdot\hat{\mathbf{p}})f^1(\mathbf{k}, p, \hat{\mathbf{p}}) - \frac{\dot{a}}{a}p\frac{\partial}{\partial p}f^1(\mathbf{k}, p, \hat{\mathbf{p}}) - \frac{1}{2}\frac{\partial f^0(p)}{\partial p}p\,\hat{\mathbf{p}}^i\hat{\mathbf{p}}^j\frac{\partial}{\partial t}h_{ij}(\mathbf{k}) = C(\mathbf{k}, p, \hat{\mathbf{p}}). \tag{4.23}$$

Complete temperature and polarization equations are derived by applying the density matrix according to the Boltzmann equation. The relationship between the Stokes parameter and the density matrix is given in Appendix 2. In the coordinate frame where $\mathbf{k} \parallel \hat{\mathbf{z}}$, the Stokes parameters depend on the angle between the photon direction and wavevector, $\mu = \hat{\mathbf{n}}\cdot\hat{\mathbf{k}}$. We will denote the fractional temperature anisotropy δT with $\Delta_T(\tau, k, \mu)$ and polarizations with $Q = \Delta_Q(\tau, k, \mu)$ and $U = \Delta_U(\tau, k, \mu)$, respectively. Their evolution equations are given by [77]

$$\begin{aligned}
\Delta_T(\tau, \hat{\mathbf{n}}, \mathbf{k}) &= \left[(1-\mu^2)e^{2i\phi}\xi^L(\mathbf{k}) + (1-\mu^2)e^{-2i\phi}\xi^R(\mathbf{k})\right]\tilde{\Delta}_T(\tau, \mu, k) \\
(\Delta_Q + i\Delta_U)(\tau, \hat{\mathbf{n}}, \mathbf{k}) &= \left[(1-\mu^2)e^{2i\phi}\xi^L(\mathbf{k}) + (1+\mu^2)e^{-2i\phi}\xi^R(\mathbf{k})\right]\tilde{\Delta}_P(\tau, \mu, k) \\
(\Delta_Q - i\Delta_U)(\tau, \hat{\mathbf{n}}, \mathbf{k}) &= \left[(1+\mu^2)e^{2i\phi}\xi^L(\mathbf{k}) + (1-\mu^2)e^{-2i\phi}\xi^R(\mathbf{k})\right]\tilde{\Delta}_P(\tau, \mu, k),
\end{aligned} \tag{4.24}$$

where $\tilde{\Delta}_T$ and $\tilde{\Delta}_P$ are variables introduced by Polnarev [87] satisfying

$$\begin{aligned}
&\tilde{\Delta}_T' + ik\mu\tilde{\Delta}_T = -h' - \kappa'\left(\tilde{\Delta}_T - \Psi\right) \\
&\tilde{\Delta}_P' + ik\mu\tilde{\Delta}_P = -\kappa'\left(\tilde{\Delta}_T + \Psi\right) \\
&\Psi \equiv \frac{1}{10}\tilde{\Delta}_{T0} + \frac{1}{7}\tilde{\Delta}_{T2} + \frac{3}{70}\tilde{\Delta}_{T4} - \frac{3}{5}\tilde{\Delta}_{P0} + \frac{6}{7}\tilde{\Delta}_{T4} - \frac{3}{70}\tilde{\Delta}_{T4},
\end{aligned} \tag{4.25}$$

where primes $'$ indicate derivatives taken with respect to the conformal time τ and h is the gravitational wave amplitude defined by

$$h_{ij}(\mathbf{x},\tau) = a^2 \sum_{m=L,R} \int d^3k e^{i\mathbf{k}\cdot\mathbf{x}} \xi^m(\mathbf{k}) e^m_{ij}(\mathbf{k}) h_k(\tau). \tag{4.26}$$

For convenience we work with right- and left- handed circularly polarized modes with polarization tensor e^L_{ij} and e^R_{ij}. The ξs are independent random variables used to characterize the statistics of the gravity waves so that

$$\begin{aligned}
&\left\langle \xi^{L*}(\mathbf{k}_1)\xi^L(\mathbf{k}_2)\right\rangle = \left\langle \xi^{R*}(\mathbf{k}_1)\xi^R(\mathbf{k}_2)\right\rangle = \frac{P_h(k)}{2}\delta(\mathbf{k}_1 - \mathbf{k}_2) \\
&\left\langle \xi^{L*}(\mathbf{k}_1)\xi^R(\mathbf{k}_2)\right\rangle = 0,
\end{aligned} \tag{4.27}$$

where $P_h(k)$ is the primordial power spectrum of the gravity waves. They are related to the original + and × polarizations by

$$\begin{aligned}
\xi^L &= \frac{1}{\sqrt{2}}(\xi^+ + i\xi^\times) \\
\xi^R &= \frac{1}{\sqrt{2}}(\xi^+ - i\xi^\times).
\end{aligned} \tag{4.28}$$

In the coordinates in which $\mathbf{k} \| \mathbf{z}$, the polarization tensors are given by

$$e_{11}(\hat{\mathbf{k}}, L/R) = -e_{22}(\hat{\mathbf{k}}, L/R) = \frac{1}{\sqrt{2}},\ e_{12}(\hat{\mathbf{k}}, L/R) = e_{21}(\hat{\mathbf{k}}, L/R) = \frac{\pm i}{\sqrt{2}}. \tag{4.29}$$

In massive gravity, the evolution of the gravitational wave amplitude is derived from the

generalized Einstein field equation [44, 43]

$$
\begin{aligned}
&h_k(\tau)'' + 2\mathcal{H}\, h_k(\tau)' + (k^2 + m_g^2 a^2)\, h_k(\tau) = 0 \\
&\ddot{h}_k(t) + 3H\, \dot{h}_k(t) + (\frac{k^2}{a^2} + m_g^2)h = 0,
\end{aligned}
\tag{4.30}
$$

where the first equation is given with respect to the conformal time, whereas the second is given with respect to physical time, $\mathcal{H}(\tau) = \frac{a'}{a}$ and $H(t) = \frac{\dot{a}}{a}$. In conventional cosmological perturbation theory, where $m_g = 0$, the solution of the above equations for a radiation-dominated universe with $a \propto \tau$, hence $a'' = 0$, is given by

$$
h_k(\tau) = \frac{1}{\tau}(C_1\, \sin(k\tau) + C_2 \cos(k\tau)). \tag{4.31}
$$

For wavelength larger than the Hubble scale, $k\tau \ll 1$, the gravitational wave amplitude is constant, while the short wavelength decays in inverse proportion to the scale factor. This is a general result valid for any equation of state. As a result, in the power spectra pattern there is a plateau for low l which corresponds to the large scale structure and drop off for $l > 100$ which corresponds to the horizon scale at recombination.

In the massive gravity case, the above equation implies that in the long wavelength limit, the amplitude of gravitational wave will oscillate with a frequency equal to m_g when the expansion rate H drops below the graviton mass. In the short wavelength limit $\frac{k}{a_{rec}} > m_g$, the evolution of gravitational wave is not affected by the graviton mass and leads to the same spectra as in the massless case. On the other hand if the graviton mass is very large, $m_g \gg H(\tau_{rec})$, the power spectra would be suppressed. We will focus on the numerical results in the following section.

4.4 Numerical results

Consider first a graviton mass below the Hubble rate during recombination, $m_g \ll H(\tau_{rec})$. Short wavelength modes, $\frac{k}{\tau_{rec})} \gg m_g$, will not be affected and have the same spectra as the massless case. Long wavelength modes, $\frac{k}{a(\tau_{rec})} \leq m_g$, which correspond to large scale structures will be modified as m_g can not be neglected. In terms of multipole

number l, short wavelength modes correspond to large l whereas long wavelength modes contribute to the low l part. We can quantify this relation using the angular size of the perturbation from recombination as observed today, $\Delta\theta$:

$$\begin{aligned} l \approx \frac{\pi}{\Delta\theta} \quad &= \pi(\frac{\lambda}{a(\tau_{rec})r_{rec}})^{-1} \\ &= \pi(\frac{\lambda}{a(\tau_0 - r_{rec})\, r_{rec}})^{-1} \\ &\approx \pi(\frac{\lambda}{a(\tau_0)\, r_{rec}})^{-1} \\ &\approx k(\tau_0 - \tau_{rec}), \end{aligned} \tag{4.32}$$

where we have used the fact that the conformal time $\tau_{rec} = \tau_0 - r_{rec}$ and r_{rec} is the comoving radial distance of the perturbation during recombination in a flat FRW universe. Then the transition to the massless regime corresponds to

$$\begin{aligned} l \gg l_0 \quad &= m_g a(\tau_{rec})(\tau_0 - \tau_{rec}) \\ &= \frac{m_g}{H_0}(1+z_{rec})^{-1} \int_{(1+z_{rec})^{-1}}^{1} \frac{dx}{\Omega_\Lambda x^4 + \Omega_m x + \Omega_r} \\ &\approx 3.3(1+z_{rec})^{-1}\frac{m_g}{H_0}, \end{aligned} \tag{4.33}$$

where we have used Planck 2013 results [2] for cosmological parameters and $z_{rec} = 1088$. We find that for graviton mass as low as $300H_0$, in which case $l_0 \approx 1$, the power spectra with massive graviton is then the same as the massless case. Hence we can not distinguish a graviton mass below this value from CMB polarization.

In this project we use the online available Code for Anisotropies in the Microwave Background (CAMB) [27, 48, 74, 75] to calculate all power spectra with the evolution equation for tensor perturbation modified according to equation 4.30. Numerical techniques CAMB uses involve second order derivatives of the source function, in which the gravitational wave amplitude is oscillating with frequency m_g for low l, therefore the numerical results from CAMB are not reliable for low l. The position of l_c, to the left of which the numerical results are not reliable, depends on the mass of gravitons and on the type of spectrum. To

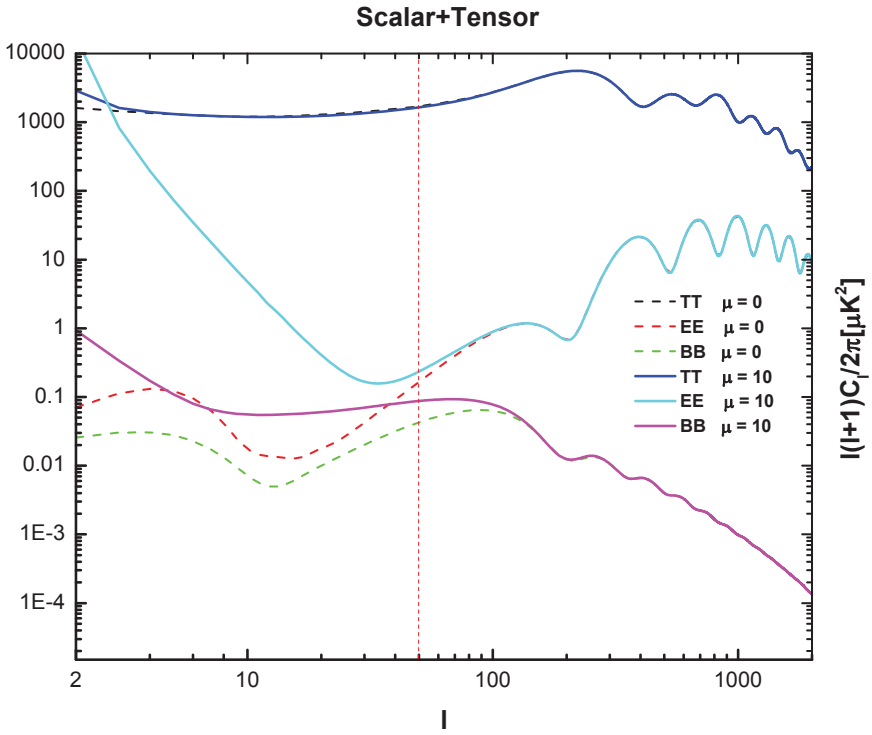

Figure 4.5. *Plot of the total $C_{TT,l}$, $C_{EE,l}$ and $C_{BB,l}$ multipole coefficients for the massless case and a moderate graviton mass. Dashed lines are for the massles case whereas solid lines are for massive gravitons. The masses are given by $m_g = \mu \times 3000H_0$, where μ is given in the legend. They are for a scalar amplitude $\Delta^2_{\mathcal{R}} = 2.2154 \times 10^{-9}$, a tensor to scalar ratio, $r = 0.1$ and a tensor spectral index $n_t = 0$. All other remaining cosmological parameters for the background, we use Planck 2013 results [2]. The vertical dashed red line indicates the position of l to the left of which the numerical calculations for massive graviton are not reliable.*

evade this numerical problem, another approach is introduced in [42] for low l range, which has second order derivatives on Bessel functions instead of having second order derivatives on the rapid oscillating source function as is used in CAMB. They differs from CAMB by integration by parts. By comparing these two approaches, the position of l_c can be found for each graviton mass and each power spectrum. According to [42], for $l > 50$ CAMB results are reliable for all spectra. For B modes auto correlation, this value could be smaller. Since this problem only exists when the graviton mass is massive, in numerical plots we show results for l ranging from 2 to 2500. We use a vertical red dashed line to indicate the position of l_c, to the left of which plots with massive graviton are not reliable. Plots for the B mode polarization are better than E modes and they reliable for $l > 30$.

In all plots we have used the scalar amplitude $\Delta^2_{\mathcal{R}} = 2.21545 \times 10^{-9}$ and set the tensor

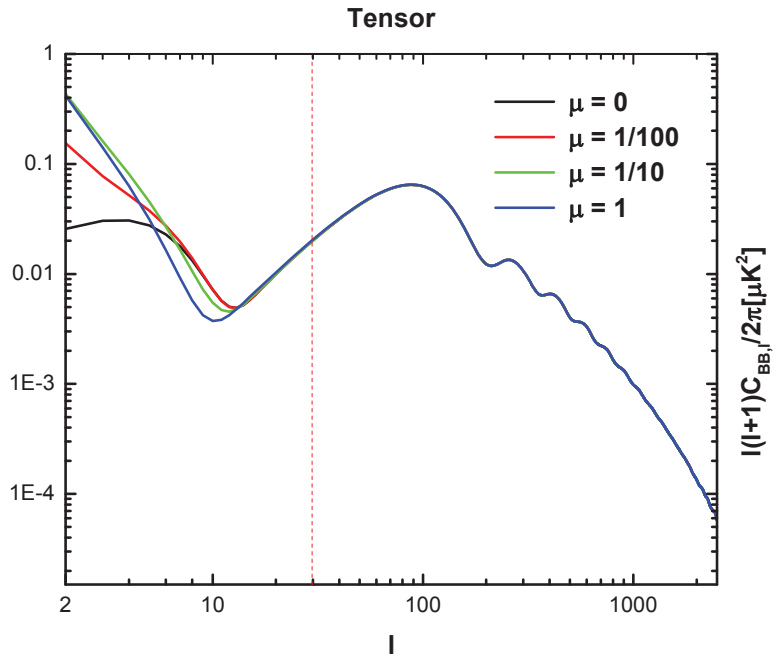

Figure 4.6. *Plot of the $C_{BB,l}$ multipole coefficients for masses below the Hubble rate during recombination. All parameters except the graviton mass are the same as Figure 4.5. The vertical dashed red line indicates the position of l_c to the left of which the numerical calculations for massive graviton are not reliable.*

to scalar ratio, r, to 0.1 as implied by Planck [2]. First we show the temperature auto correlation, E mode auto correlation and B modes auto correlation for both the massless case and a nonzero moderate massive graviton in one Figure 4.5, which are from both scalar and tensor perturbations. The upper curve (dashed black for massless graviton and solid blue for massive graviton) is the most familiar temperature anisotropy spectrum, with amplitudes 5 orders of magnitude smaller than the CMB temperature of $2.7K$. The polarization signals (EE and BB) are smaller by an additional $1 \backsim 2$ orders of magnitude because they are produced by the quadruple component of the temperature fluctuations at recombination. They reach a maximum around $l \approx 100$, corresponding to the horizon scale at recombination, and drop off for $l < 100$, corresponding to the superhorizon scales. B modes decreases on subhorizon scales, $l > 100$, due to the decrease of gravitational amplitude on small scales as can be seen from equation 4.30. Dashed lines correspond to the massless case and solid lines represent the modification by a moderate graviton mass which is a little above the Hubble

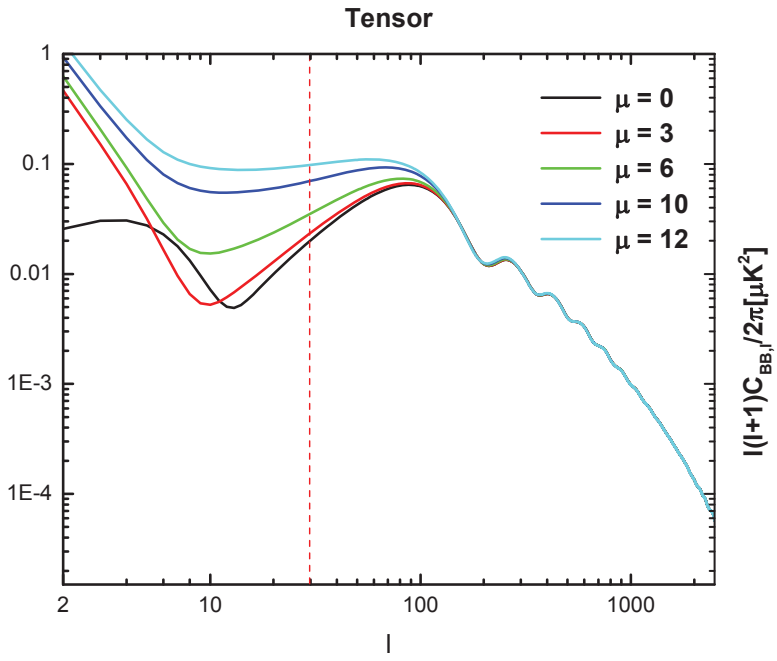

Figure 4.7. *Plot of the $C_{BB,l}$ multipole coefficients for masses around the Hubble rate during recombination. The masses are given by $m_g = \mu \times 3000 H_0$, where μ is given in the legend. All parameters except the graviton mass are the same as Figure 4.5. The vertical dashed red line indicates the position of l_c to the left of which the numerical calculations for massive graviton are not reliable.*

rate during recombination, $m_g = 3 \times 10^4 H_0$. The effect on temperature and E modes power spectra is not obvious as their main contributions are from scalar perturbations which remain the same with a massive graviton in our consideration. The B modes spectrum is enhanced with this graviton mass compared to the massless case. Therefore from now on we will only focus on B modes.

For masses below the Hubble rate during recombination $H(\tau_{rec}) \approx 2 \times 10^4 H_0$ or $\mu < 7$, the effect of a graviton mass is rather mild and is present for very low l [42, 92]. In our numerical calculation for $l > 50$ in Figure 4.6, no effect is observed. This is in agreement with our earlier qualitative analysis.

For masses approaching the Hubble rate during recombination or a little higher, the signature of a graviton mass on the B polarization is obvious. As shown in figure 4.7, the power spectra are enhanced by a graviton mass compared to the massless case. In the plot,

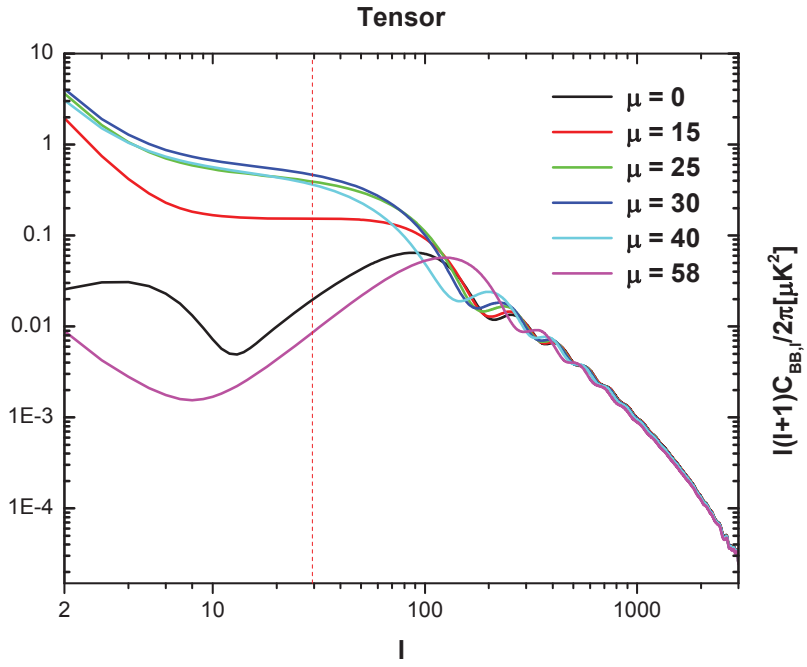

Figure 4.8. *Plot of the $C_{BB,l}$ multipole coefficients for masses above the Hubble rate during recombination. The masses are given by $m_g = \mu \times 3000 H_0$, where μ is given in the legend. All parameters except the graviton mass are the same as Figure 4.5. The vertical dashed red line indicates the position of l_c to the left of which the numerical calculations for massive graviton are not reliable.*

the black line represents the massless case and the colored lines represent different graviton masses. The greater the graviton mass, the higher the power spectra, and they approach to a plateau in agreement with [42]. The height of the plateau will continue to increase until the graviton mass goes up to $\mu = 30$, then it starts to decrease as can be seen in Figures 4.8. This is a bit different from [42], in which it happens at $\mu = 25$. This is because we used Planck 2013 results [2] for the cosmological parameters of the background, whereas [42] used WMAP values [12].

For μ larger than 30, we find that the height of the plateau goes down and up followed by two minimum at $\mu = 56$ and 100, which are suppressed compared to the massless case, and two peaks at $\mu = 78$ and $\mu = 120$, which are lower than that when $\mu = 30$. This is shown in figure 4.9. Two upper solid lines represent the two maximum for the plateau, while the two lower dashed lines correspond to two minimum of the plateau. For $l > 100$ the

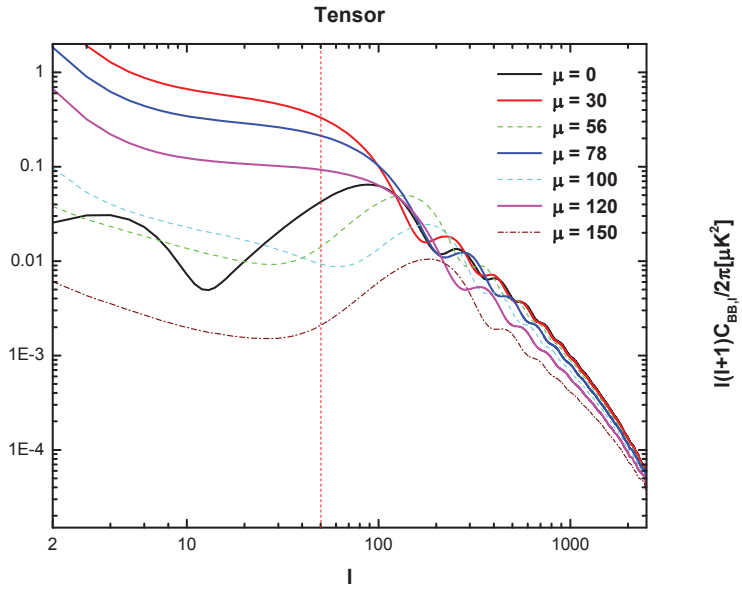

Figure 4.9. *Plot of the $C_{BB,l}$ multipole coefficients for masses above the Hubble rate during recombination. The masses are given by $m_g = \mu \times 3000 H_0$, where μ is given in the legend. All parameters except the graviton mass are the same as Figure 4.5. The vertical dashed red line indicates the position of l_c to the left of which the numerical calculations for massive graviton are not reliable.*

plateau decreases with increasing graviton mass. For $\mu > 140$, the polarization pattern is suppressed compared to the massless case due to the rapid oscillation of tensor perturbations during recombination as we see in equation 4.30. For graviton mass $\mu = 200$ as shown in Figure 4.10, the power spectrum is one order less than the massless case. Higher masses are suppressed more, as shown by the blue line which corresponds to $\mu = 1000$.

We also plotted the temperature spectrum in figure 4.11, E modes in figure 4.13 and the cross correlation between them in figure 4.14 from tensor perturbations only for graviton mass $\mu = 10$ in comparison with the B mode polarization in figure 4.12. We find that the temperature anisotropy is suppressed for a moderate graviton mass compared to the massless case as shown in figure 4.11. This is different from polarization auto correlation, as both E modes and B modes are enhanced for this graviton mass as shown in figures 4.13 and 4.12.

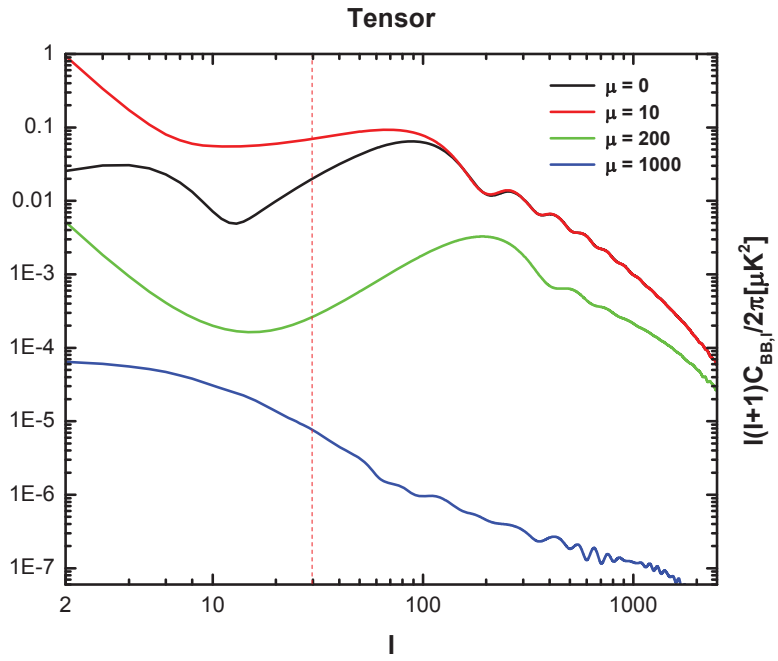

Figure 4.10. *Plot of the $C_{BB,l}$ multipole coefficients for masses above the Hubble rate during recombination. The masses are given by $m_g = \mu \times 3000 H_0$, where μ is given in the legend. All parameters except the graviton mass are the same as Figure 4.5. The vertical dashed red line indicates the position of l_c to the left of which the numerical calculations for massive graviton are not reliable.*

Due to the suppressed temperature, the cross correlation between temperature and E modes is also suppressed for this particular graviton mass as shown in figure 4.14.

We did not analyze more results about temperature and E modes, since their main contributions are from scalar perturbations, which are independent on the graviton mass. B modes are more interesting since scalar modes do not generate them and vector modes decay during cosmic expansion. This makes the study of B mode polarization quite important in the study of gravitational waves.

4.5 Summary

In this project, we studied the effect of a graviton mass on B modes polarization. We find that a moderate graviton mass, about the order of the Hubble rate during recombination $H(\tau_{rec}) = 2 \times 10^4 H_0$, would enhance the power spectra and leads to a characteristic plateau for $l < 100$. The height of the plateau increases until μ reaches 30, then it starts to decrease.

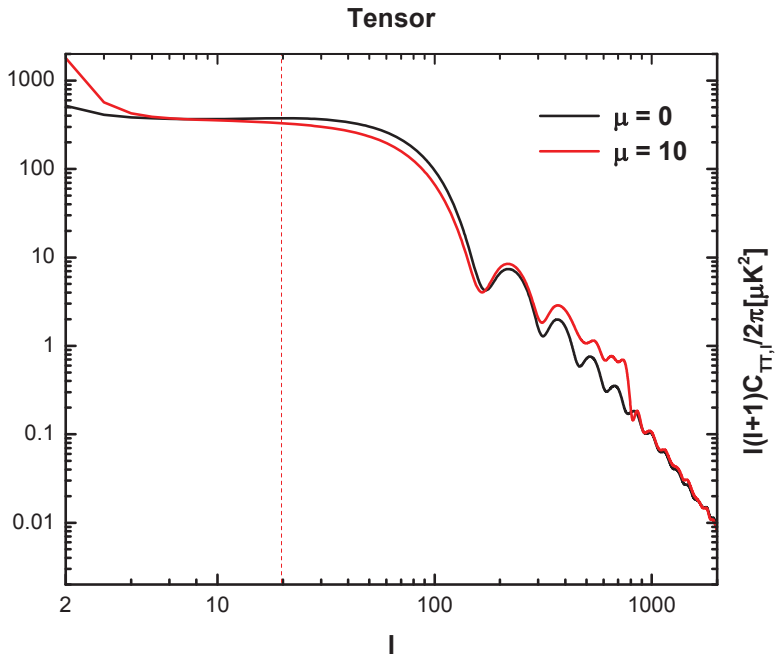

Figure 4.11. *Plot of the T spectra for the massive case $\mu = 10$ (red line) and for the massless case (black line). All parameters except the graviton mass are the same as Figure 4.5. The vertical dashed red line indicates the position of l_c to the left of which the numerical calculations for massive graviton are not reliable.*

It reaches a minimum at $\mu = 56$ and goes up again with increasing graviton mass. There are two secondary maxima at $\mu = 78$ and $\mu = 120$, lower than that at $\mu = 30$, and two minima at $\mu = 56$ and $\mu = 100$, which are suppressed compared to the massless case. A large graviton mass would make long wavelength modes oscillate with the same frequency given by the graviton mass and hence suppresses the polarization considerably. By comparing to the massless case, we find that B modes polarization could provide a tight constraint on graviton mass $m_g \lesssim 10^{-30}$eV. In the general case when the graviton mass is time varying [56], this constraint is put on graviton mass during recombination. This is because the polarization was generated by tensor perturbations during recombination and then carried by decoupled photons traveling to us freely since then. We find that a graviton mass in the range $10^{-30}\text{eV} \lesssim m_g \lesssim 10^{-27}\text{eV}$ would lead to interesting modifications on the CMB power spectra especially the B modes polarization. Results are in agreement with [42].

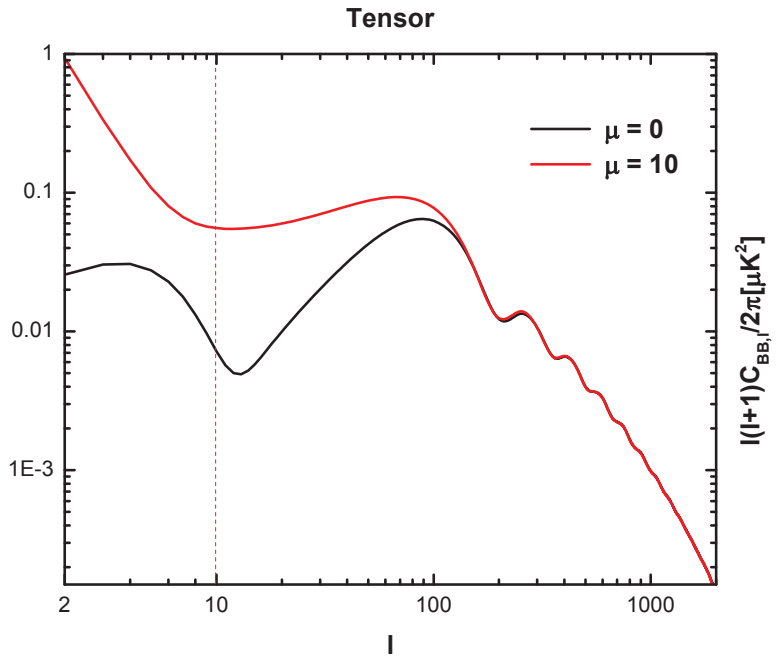

Figure 4.12. *Plot of the T spectra for the massive case $\mu = 10$ (red line) and for the massless case (black line). All parameters except the graviton mass are the same as Figure 4.5. The vertical dashed red line indicates the position of l_c to the left of which the numerical calculations for massive graviton are not reliable.*

Since current polarization measurements are getting unprecedented high level of sensitivity, detection of B modes polarization is expected in the near future. A detection of power spectra with this signature will be strong proof for the existence of graviton mass.

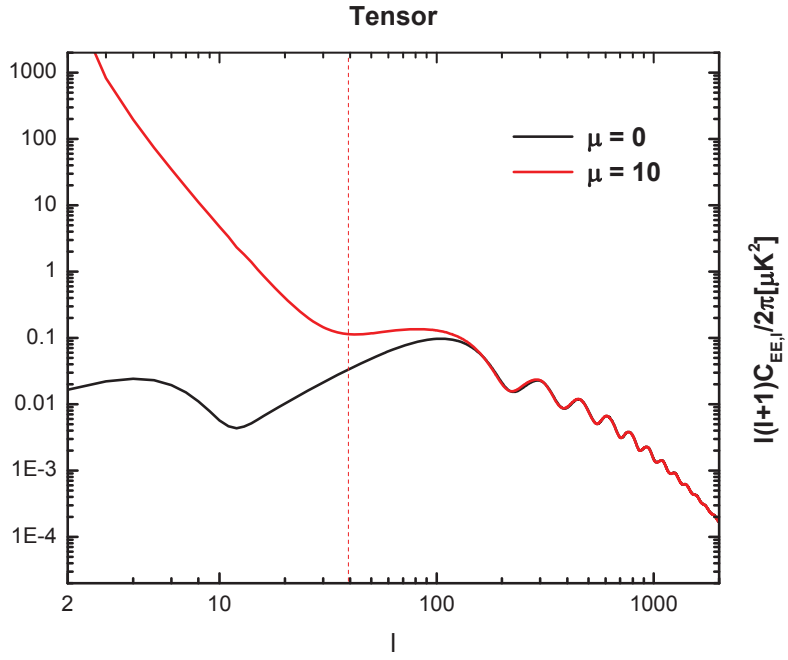

Figure 4.13. *Plot of the E spectra for the massive case* $\mu = 10$ *(red line) and for the massless case (black line). All parameters except the graviton mass are the same as Figure 4.5. The vertical dashed red line indicates the position of* l_c *to the left of which the numerical calculations for massive graviton are not reliable.*

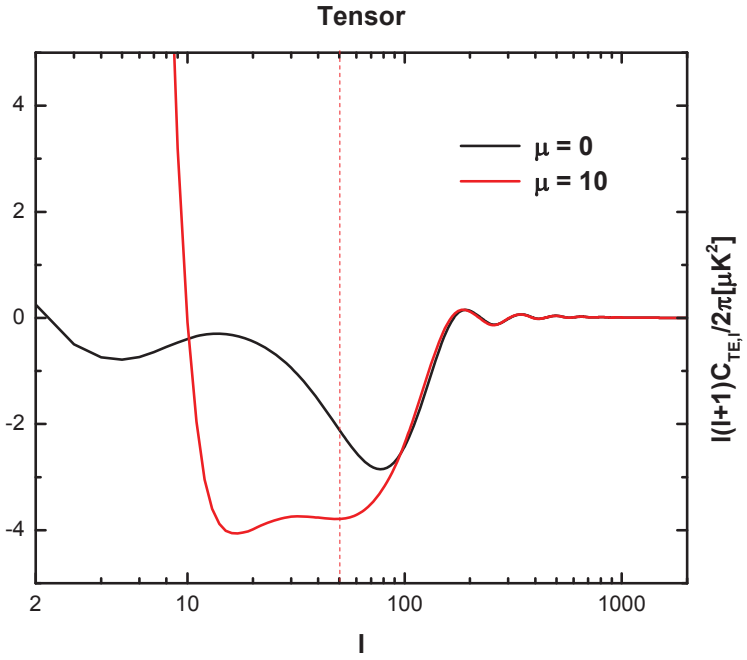

Figure 4.14. *Plot of the TE spectra for the massive case $\mu = 10$ (red line) and for the massless case (black line). All parameters except the graviton mass are the same as Figure 4.5. The vertical dashed red line indicates the position of l_c to the left of which the numerical calculations for massive graviton are not reliable.*

This Page Intentionally Left Blank

A.1 Natural units

In Chapter 4 we adopt natural units, in which $c = 1$, $\hbar = 1$ and $k_B = 1$. We use Mpc as a unit of length, time and inverse energy. Here are some fundamental constants of nature

$$\begin{aligned}
&\text{Planck's constant} \quad \hbar = 1.0546 \times 10^{-27}\,\mathrm{cm^2 g\,s^{-1}} \\
&\text{Speed of light} \quad c = 2.9979 \times 10^{10}\,\mathrm{cm\,s^{-1}} \\
&\text{Thomson cross section} \quad \sigma_{\mathrm{T}} = 8\pi\alpha^2/3\mathrm{m_e^2} = 6.6524 \times 10^{-25}\,\mathrm{cm^2} \\
&\text{Electron mass} \quad m_e = 0.5110\,\mathrm{MeV} \\
&\text{Proton mass} \quad m_p = 938.272\,\mathrm{MeV} \\
&\text{Neutron mass} \quad m_n = 939.566\,\mathrm{MeV} \\
&\text{Planck mass} \quad m_{pl} = \mathrm{G}^{1/2} = 1.221 \times 10^{19}\,\mathrm{GeV}
\end{aligned} \tag{34}$$

Here are some unit conversions

$$\begin{aligned}
1\,\mathrm{s} &= 9.7157 \times 10^{-15}\,\mathrm{Mpc} \\
1\,\mathrm{yr} &= 3.1558 \times 10^{7}\,\mathrm{s} \\
1\,\mathrm{Mpc} &= 3.0856 \times 10^{22}\,\mathrm{m} \\
&= (6.4 \times 10^{-30}\,\mathrm{eV})^{-1} \\
1\,\mathrm{AU} &= 1.4960 \times 10^{11}\,\mathrm{m} \\
1\,\mathrm{GeV} &= 1.6022 \times 10^{-3}\,\mathrm{erg} \\
&= 1.7827 \times 10^{-24}\,\mathrm{g} \\
&= (1.9733 \times 10^{-14}\,\mathrm{cm})^{-1} \\
&= (6.5821 \times 10^{-25}\,\mathrm{s})^{-1}
\end{aligned} \tag{35}$$

The Hubble constant is given by

$$\begin{aligned} H_0 &= 67.8\,\mathrm{km/sec/Mpc} \\ &= (4.42\times 10^3\,\mathrm{Mpc})^{-1} \\ &= 1.45\times 10^{-33}\,\mathrm{eV} \end{aligned} \tag{36}$$

A.2 The Boltzmann equation

To understand the time evolution of stokes parameters, we also introduce their quantum mechanical definition in terms of the density matrix

$$\rho = \frac{1}{2}\begin{pmatrix} I+Q & U-iV \\ U+iV & I-Q \end{pmatrix}.$$

The Boltzmann equation is given by

$$\begin{aligned} \frac{d}{d\,t}\rho_{ij}(\mathbf{x},\mathbf{k}) &= \frac{\epsilon^4 n_e(\mathbf{x})}{16\pi m_e^2 k}\int_0^\infty d\,p\;p\int\frac{d\Omega}{4\pi}\big[\delta(k-p)+(\mathbf{k}-\mathbf{p})\cdot\mathbf{v}(\mathbf{x})\frac{\partial\delta(k-p)}{\partial p}\big] \\ &\times\{-2(\frac{p}{k}+\frac{k}{p})\rho_{ij}(bfx,k)+4\hat{\mathbf{p}}\cdot\hat{\epsilon}_i(\mathbf{k})\hat{\mathbf{p}}\cdot\hat{\epsilon}_1(\mathbf{k})\rho_{1j}(\mathbf{x},\mathbf{k}) \\ &+4\hat{\mathbf{p}}\cdot\hat{\epsilon}_i(\mathbf{k})\hat{\mathbf{p}}\cdot\hat{\epsilon}_2(\mathbf{k})\rho_{2j}(\mathbf{x},\mathbf{k}) \\ &+(\frac{p}{k}+\frac{k}{p}-2)\delta_{ij}(\rho_{11}(\mathbf{x},\mathbf{p})+\rho_{22}(\mathbf{x},\mathbf{p})) \\ &+(\frac{p}{k}+\frac{k}{p})(\epsilon_i(\mathbf{k})\cdot\epsilon_1(\mathbf{p})\epsilon_j(\mathbf{k})\cdot\epsilon_2(\mathbf{p})-\epsilon_i(\mathbf{k})\cdot\epsilon_2(\mathbf{p})\epsilon_j(\mathbf{k})\cdot\epsilon_1(\mathbf{p})(\rho_{12}(\mathbf{x},\mathbf{p})-\rho_{21}(\mathbf{x},\mathbf{p})) \\ &+2(\epsilon_i(\mathbf{k})\cdot\epsilon_1(\mathbf{p})\epsilon_j(\mathbf{k})\cdot\epsilon_2(\mathbf{p})+\epsilon_i(\mathbf{k})\cdot\epsilon_2(\mathbf{p})\epsilon_j(\mathbf{k})\cdot\epsilon_1(\mathbf{p}))(\rho_{12}(\mathbf{x},\mathbf{p})+\rho_{21}(\mathbf{x},\mathbf{p})) \\ &+4\epsilon_i(\mathbf{k})\cdot\epsilon_1(\mathbf{p})\epsilon_j(\mathbf{k})\cdot\epsilon_1(\mathbf{p})\rho_{11}(\mathbf{x},\mathbf{p})+4\epsilon_i(\mathbf{k})\cdot\epsilon_2(\mathbf{p})\epsilon j_(\mathbf{k})\cdot\epsilon_2(\mathbf{p})\rho_{22}(\mathbf{x},\mathbf{p})\} \end{aligned} \tag{37}$$

where $\mathbf{p}$ is the 3-d momentum vector incoming photons from all direction before collision with electrons, $\mathbf{k}$ is the the 3-d momentum vector of the outgoing photons after collision moving toward observers, ϵ_i are polarization vectors with i running through 1 to 2.

In spherical coordinates, the basis for the photon direction and polarization vectors is taken to be

$$\begin{aligned}
&\hat{\mathbf{k}}_x = \sin\theta\cos\phi,\ \ \hat{\mathbf{k}}_y = \sin\theta\sin\phi,\ \ \hat{\mathbf{k}}_z = \cos\theta \\
&\hat{\epsilon}_{1x}(\mathbf{k}) = \cos\theta\cos\phi,\ \ \hat{\epsilon}_{1y}(\mathbf{k}) = \cos\theta\ \sin\phi,\ \ \hat{\epsilon}_{1z}(\mathbf{k}) = -\sin\theta \\
&\hat{\epsilon}_{2x} = -\sin\phi,\ \ \hat{\epsilon}_{2y} = \cos\phi,\ \ \hat{\epsilon}_{2z}(\mathbf{k}) = 0.
\end{aligned} \tag{38}$$

A.3 Spin weighted functions

For any given direction on the sphere specified by angles (θ, ϕ), we can define three orthogonal vectors, one radial $\hat{\mathbf{n}}$ and the other two tangential to the sphere labeled as $\hat{\mathbf{e}}_1$ and $\hat{\mathbf{e}}_2$.

A function defined on the sphere is said to have spin s if under a right handed rotation on the plane normal to $\hat{\mathbf{n}}$ by angle ψ, it transforms as ${}_sf'(\theta,\phi) = e_s^{-is\psi} f(\theta,\phi)$. There exist spin-s spherical harmonics ${}_sY_{lm}(\theta,\phi)$ [53, 83, 111]

$$\begin{aligned}
{}_sY_{lm}(\hat{\mathbf{n}}) = \quad & e^{im\phi}\big[\frac{(l+m)!(l-m)!}{(l+s)!(l-s)!}\frac{2l+1}{4\pi}\big]^{1/2}\sin^{2l}(\theta/2) \\
& \times\sum_r \binom{l-s}{r}\binom{l+s}{r+s-m}(-1)^{l-r-s+m}\cot^{2r+s-m}(\theta/2),
\end{aligned} \tag{39}$$

which are complete and orthogonal,

$$\begin{aligned}
&\int_0^{2\pi} d\phi \int_{-1}^{1} {}_sY^*_{l'm'}(\theta,\phi)\,{}_sY_{lm}(\theta,\phi) = \delta_{ll'}\delta_{mm'} \\
&\sum_{lm} {}_sY^*_{lm}(\theta,\phi)\,{}_sY_{lm}(\theta',\phi') = \delta(\phi-\phi')\delta(\cos\theta-\cos\theta').
\end{aligned} \tag{40}$$

There exist spin raising and lowering operators, $\eth$ and $\bar{\eth}$, such that they can raise or lower the spin weight of a function, $(\eth\,{}_sf)' = e^{-i(s+1)\psi}\eth_s f$, $(\bar{\eth}_s f)' = e^{-i(s-1)\psi}\bar{\eth}_s f$. Their forms are

given by

$$\eth_s f(\theta,\phi) = -\sin^s(\theta)\big[\frac{\partial}{\partial\theta} + i\csc(\theta)\frac{\partial}{\partial\phi}\big]\sin^{-s}(\theta)_s f(\theta,\phi)$$
$$\bar{\eth}_s f(\theta,\phi) = -\sin^{-s}(\theta)\big[\frac{\partial}{\partial\theta} - i\csc(\theta)\frac{\partial}{\partial\phi}\big]\sin^{s}(\theta)_s f_(\theta,\phi). \tag{41}$$

Acting twice the spin raising (lowering) operator on spin -2 (2) functions ${}_{\pm 2}f(\mu,\phi)$ with $\mu = \cos\theta$, we obtain spin 0 functions which are rotation invariant,

$$\eth^2{}_{-2}f(\mu,\phi) = \big(-\partial\mu - \frac{m}{1-\mu^2}\big)^2\big[(1-\mu^2)_{-2}f(\mu,\phi)\big]$$
$$\bar{\eth}^2{}_2 f(\mu,\phi) = \big(-\partial\mu + \frac{m}{1-\mu^2}\big)^2\big[(1-\mu^2)_2 f(\mu,\phi)\big]. \tag{42}$$

Bibliography

Bibliography

[1] P.A.R. Ade et al. Planck 2013 results. I. Overview of products and scientific results. *Astron. Astrophys.*, 571:A1, 2014.

[2] P.A.R. Ade et al. Planck 2013 results. XVI. Cosmological parameters. *Astron. Astrophys.*, 571:A16, 2014.

[3] Nima Arkani-Hamed, Howard Georgi, and Matthew D. Schwartz. Effective field theory for massive gravitons and gravity in theory space. *Annals Phys.*, 305:96–118, 2003.

[4] K.G. Arun and Clifford M. Will. Bounding the mass of the graviton with gravitational waves: Effect of higher harmonics in gravitational waveform templates. *Class. Quant. Grav.*, 26:155002, 2009.

[5] Eugeny Babichev and Alessandro Fabbri. Instability of black holes in massive gravity. 2013.

[6] Eugeny Babichev and Alessandro Fabbri. A class of charged black hole solutions in massive (bi)gravity. *JHEP*, 1407:016, 2014.

[7] Eugeny Babichev and Alessandro Fabbri. Rotating black holes in massive gravity. *Phys. Rev.*, D90:084019, 2014.

[8] Eugeny Babichev and Alessandro Fabbri. Stability analysis of black holes in massive gravity: a unified treatment. *Phys. Rev.*, D89:081502, 2014.

[9] J. Bardeen. Gauge Invariant Cosmological Perturbations. *Phys. Rev.*, D22:1882–1905, 1980.

[10] D. Baskaran, L.P. Grishchuk, and A.G. Polnarev. Imprints of Relic Gravitational Waves in Cosmic Microwave Background Radiation. *Phys. Rev.*, D74:083008, 2006.

[11] Michael V. Bebronne and Peter G. Tinyakov. Massive gravity and structure formation. *Phys. Rev.*, D76:084011, 2007.

[12] C.L. Bennett, R.S. Hill, G. Hinshaw, D. Larson, K.M. Smith, et al. Seven-Year Wilkinson Microwave Anisotropy Probe (WMAP) Observations: Are There Cosmic Microwave Background Anomalies? *Astrophys. J. Suppl.*, 192:17, 2011.

[13] L. Berezhiani, G. Chkareuli, C. de Rham, G. Gabadadze, and A.J. Tolley. On Black Holes in Massive Gravity. *Phys. Rev.*, D85:044024, 2012.

[14] Emanuele Berti, Alessandra Buonanno, and Clifford M. Will. Estimating spinning binary parameters and testing alternative theories of gravity with LISA. *Phys. Rev.*, D71:084025, 2005.

[15] Emanuele Berti, Jonathan Gair, and Alberto Sesana. Graviton mass bounds from space-based gravitational-wave observations of massive black hole populations. *Phys. Rev.*, D84:101501, 2011.

[16] Edmund Bertschinger. Cosmological perturbation theory and structure formation. pages 1–25, 2001.

[17] Dennis Bessada and Oswaldo D. Miranda. CMB Polarization and Theories of Gravitation with Massive Gravitons. *Class. Quant. Grav.*, 26:045005, 2009.

[18] J. Bij, H. Dam, and Y. Ng. The exchange of massless spin-two particles. *Physica*, 116A:307–320, 1982.

[19] Luc Blanchet and B.S. Sathyaprakash. Signal analysis of gravitational wave tails. *Class. Quant. Grav.*, 11:2807–2832, 1994.

[20] Luca Bombelli. Unimodular relativity, general covariance, time, and the Ashtekar variables. *Banff 1990, Proceedings, Gravitation*, pages 221–232, 1990.

[21] Luca Bombelli, W. E. Couch, and R. J. Torrence. Time as spacetime four-volume and the Ashtekar variables. *Phys. Rev.*, D44:2589, 1991.

[22] D.G. Boulware and Stanley Deser. Can gravitation have a finite range? *Phys. Rev.*, D6:3368–3382, 1972.

[23] Robert H. Brandenberger. Introduction to Early Universe Cosmology. *PoS*, ICFI2010:001, 2010.

[24] Richard Brito, Vitor Cardoso, and Paolo Pani. Massive spin-2 fields on black hole spacetimes: Instability of the Schwarzschild and Kerr solutions and bounds on the graviton mass. *Phys. Rev.*, D88(2):023514, 2013.

[25] R. W. Hellings C. Talmadge, J. P. Berthias and E. M. Standish. Model-Independent Constraints on Possible Modifications of Newtonian Gravity. *Phys. Rev. Lett.*, 61:1159, 1988.

[26] Yi-Fu Cai, Damien A. Easson, Caixia Gao, and Emmanuel N. Saridakis. Charged black holes in nonlinear massive gravity. *Phys. Rev. D 87,*, 064001, 2013.

[27] Anthony Challinor. Microwave background anisotropies from gravitational waves: The (1+3) covariant approach. *Class. Quant. Grav.*, 17:871–889, 2000.

[28] Anthony Challinor. Microwave background polarization in cosmological models. *Phys. Rev.*, D62:043004, 2000.

[29] Giga Chkareuli and David Pirtskhalava. Vainshtein Mechanism In Λ_3 - Theories. *Phys. Lett.*, B713:99–103, 2012.

[30] S.R. Choudhury, Girish C. Joshi, S. Mahajan, and Bruce H.J. McKellar. Probing large distance higher dimensional gravity from lensing data. *Astropart. Phys.*, 21:559–563, 2004.

[31] Nathan Chow and Justin Khoury. Galileon Cosmology. *Phys. Rev.*, D80:024037, 2009.

[32] Timothy Clifton, Pedro G. Ferreira, Antonio Padilla, and Constantinos Skordis. Modified Gravity and Cosmology. *Phys. Rept.*, 513:1–189, 2012.

[33] D. Comelli, M. Crisostomi, F. Nesti, and L. Pilo. Spherically Symmetric Solutions in Ghost-Free Massive Gravity. *Phys. Rev.*, D85:024044, 2012.

[34] Robert Crittenden, J. Richard Bond, Richard L. Davis, George Efstathiou, and Paul J. Steinhardt. The Imprint of gravitational waves on the cosmic microwave background. *Phys. Rev. Lett.*, 71:324–327, 1993.

[35] Curt Cutler, William A. Hiscock, and Shane L. Larson. LISA, binary stars, and the mass of the graviton. *Phys. Rev.*, D67:024015, 2003.

[36] Antonio De Felice and Shinji Tsujikawa. f(R) theories. *Living Rev. Rel.*, 13:3, 2010.

[37] Claudia de Rham. Massive Gravity. *Living Rev. Rel.*, 17:7, 2014.

[38] Claudia de Rham and Gregory Gabadadze. Generalization of the Fierz-Pauli Action. *Phys. Rev.*, D82:044020, 2010.

[39] Claudia de Rham, Gregory Gabadadze, and Andrew J. Tolley. Helicity Decomposition of Ghost-free Massive Gravity. *JHEP*, 1111:093, 2011.

[40] Claudia de Rham, Gregory Gabadadze, and Andrew J. Tolley. Resummation of Massive Gravity. *Phys. Rev. Lett.*, 106:231101, 2011.

[41] Claudia de Rham, Gregory Gabadadze, and Andrew J. Tolley. Ghost free Massive Gravity in the Stúckelberg language. *Phys. Lett.*, B711:190–195, 2012.

[42] Sergei Dubovsky, Raphael Flauger, Alexei Starobinsky, and Igor Tkachev. Signatures of a Graviton Mass in the Cosmic Microwave Background. *Phys. Rev.*, D81:023523, 2010.

[43] S.L. Dubovsky. Phases of massive gravity. *JHEP*, 0410:076, 2004.

[44] S.L. Dubovsky, P.G. Tinyakov, and I.I. Tkachev. Cosmological attractors in massive gravity. *Phys. Rev.*, D72:084011, 2005.

[45] S.L. Dubovsky, P.G. Tinyakov, and I.I. Tkachev. Massive graviton as a testable cold dark matter candidate. *Phys. Rev. Lett.*, 94:181102, 2005.

[46] A. Einstein. The Principle of Relativity. *Siz. Preuss. Acad. Scis.*, page 433, 1919.

[47] G. Ellis, H. van Elst, J. Murugan, and J. Uzan. On the Trace-Free Einstein Equations as a Viable Alternative to General Relativity. *Class. Quantum. Grav.*, 28:225007, 2011.

[48] G. F. R Ellis, D. R Matravers, and R Treclokas. Anisotropic solutions of the Einstein-Boltzmann equations: I. General formalism. *Annals of Physics*, 150:455–486, 1983.

[49] M. Fierz and W. Pauli. On relativistic wave equations for particles of arbitrary spin in an electromagnetic field. *Proc. Roy. Soc. Lond.*, A173:211–232, 1939.

[50] D. Finkelstein, A. Galiautdinov, and J. Baugh. Unimodular relativity and cosmological constant. *J. Math. Phys.*, 42:340–346, 2001.

[51] Lee Samuel Finn and Patrick J. Sutton. Bounding the mass of the graviton using binary pulsar observations. *Phys. Rev.*, D65:044022, 2002.

[52] Raphael Flauger, J. Colin Hill, and David N. Spergel. Toward an Understanding of Foreground Emission in the BICEP2 Region. *JCAP*, 1408:039, 2014.

[53] J. N. Goldberg, A. J. Macfarlane, E. T. Newman, F. Rohrlich, and E. C. G. Sudarshan. Spin-s Spherical Harmonics and $\eth$. *J. Math. Phys. (American Institute of Physics)*, 8:2155 2161, 1967.

[54] Alfred S. Goldhaber and Michael Martin Nieto. Mass of the graviton. *Phys. Rev.*, D9:1119, 1974.

[55] Andrei Gruzinov and Mehrdad Mirbabayi. Stars and Black Holes in Massive Gravity. *Phys. Rev.*, D84:124019, 2011.

[56] A. Emir Gumrukcuoglu, Sachiko Kuroyanagi, Chunshan Lin, Shinji Mukohyama, and Norihiro Tanahashi. Gravitational wave signal from massive gravity. *Class. Quantum. Grav.*, 29:235026, 2012.

[57] D. Hanson et al. Detection of B-mode Polarization in the Cosmic Microwave Background with Data from the South Pole Telescope. *Phys. Rev. Lett.*, 111(14):141301, 2013.

[58] S.F. Hassan and Rachel A. Rosen. On Non-Linear Actions for Massive Gravity. *JHEP*, 1107:009, 2011.

[59] Kurt Hinterbichler. Theoretical Aspects of Massive Gravity. *Rev. Mod. Phys.*, 84:671–710, 2012.

[60] Wayne Hu and Scott Dodelson. Cosmic microwave background anisotropies. *Ann. Rev. Astron. Astrophys.*, 40:171–216, 2002.

[61] Wayne Hu and Martin J. White. A CMB polarization primer. *New Astron.*, 2:323, 1997.

[62] John David Jackson. *Classical Electrodynamics* , 1998.

[63] P. Jain, A. Jaiswal, P. Karmakar, G. Kashyap, and N. Singh. Cosmological implications of unimodular gravity. *JCAP*, 1211:003, 2012.

[64] Soumya Jana. Cosmology in a reduced Born-Infeld–$f(T)$ theory of gravity. *Phys. Rev.*, D90:124007, 2014.

[65] Marc Kamionkowski, Arthur Kosowsky, and Albert Stebbins. A Probe of primordial gravity waves and vorticity. *Phys. Rev. Lett.*, 78:2058–2061, 1997.

[66] Marc Kamionkowski, Arthur Kosowsky, and Albert Stebbins. Statistics of cosmic microwave background polarization. *Phys. Rev.*, D55:7368–7388, 1997.

[67] Brian G. Keating, Alexander G. Polnarev, Nathan J. Miller, and Deepak Baskaran. The Polarization of the Cosmic Microwave Background Due to Primordial Gravitational Waves. *Int. J. Mod. Phys.*, A21:2459–2479, 2006.

[68] Bence Kocsis, Zoltan Haiman, and Kristen Menou. Pre-Merger Localization of Gravitational-Wave Standard Sirens With LISA: Triggered Search for an Electromagnetic Counterpart. *Astrophys. J.*, 684:870–888, 2008.

[69] Hideo Kodama and Ivan Arraut. Stability of the Schwarzschildde Sitter black hole in the dRGT massive gravity theory. *PTEP*, 2014(2):023E02, 2014.

[70] Arthur Kosowsky. Cosmic microwave background polarization. *Annals Phys.*, 246:49–85, 1996.

[71] Kazuya Koyama, Gustavo Niz, and Gianmassimo Tasinato. Analytic solutions in non-linear massive gravity. *Phys. Rev. Lett.*, 107:131101, 2011.

[72] Kazuya Koyama, Gustavo Niz, and Gianmassimo Tasinato. Strong interactions and exact solutions in non-linear massive gravity. *Phys. Rev.*, D84:064033, 2011.

[73] Shane L. Larson and William A. Hiscock. Using binary stars to bound the mass of the graviton. *Phys. Rev.*, D61:104008, 2000.

[74] Antony Lewis and Sarah Bridle. Cosmological parameters from CMB and other data: A Monte Carlo approach. *Phys. Rev.*, D66:103511, 2002.

[75] Antony Lewis and Anthony Challinor. The code is available at http://camb.info.

[76] E. Lifshitz. On the Gravitational stability of the expanding universe. *J. Phys. (USSR)*, 10:116, 1946.

[77] Chung-Pei Ma and Edmund Bertschinger. Cosmological perturbation theory in the synchronous and conformal Newtonian gauges. *Astrophys. J.*, 455:7–25, 1995.

[78] Michele Maggiore. Gravitational wave experiments and early universe cosmology. *Phys. Rept.*, 331:283–367, 2000.

[79] Mehrdad Mirbabayi and Andrei Gruzinov. Black hole discharge in massive electrodynamics and black hole disappearance in massive gravity. *Phys. Rev.*, D88:064008, 2013.

[80] Taeyoon Moon and Yun Soo Myung. Gregory-Laflamme instability of the BTZ black hole in new massive gravity. *Phys. Rev.*, D88(12):124014, 2013.

[81] V. Mukhanov. *Physical foundations of cosmology*, 2005.

[82] V. Mukhanov, H.A. Feldman, and R. Brandenberger. Theory of cosmological perturbations. Part 1. Classical perturbations. Part 2. Quantum theory of perturbations. Part 3. Extensions. *Phys. Rept.*, 215:203–333, 1992.

[83] E. T. Newman and R. Penrose. Note on the Bondi-Metzner-Sachs Group. *J. Math. Phys. (American Institute of Physics)*, 7:863 870, 1966.

[84] Y. Jack Ng and H. van Dam. Unimodular Theory of Gravity and the Cosmological Constant. *J. Math. Phys.*, 32:1337–1340, 1991.

[85] Th.M. Nieuwenhuizen. Exact Schwarzschild-de Sitter black holes in a family of massive gravity models. *Phys. Rev.*, D84:024038, 2011.

[86] S. Perlmutter et al. Measurements of Omega and Lambda from 42 high redshift supernovae. *Astrophys. J.*, 517:565–586, 1999.

[87] A.G. Polnarev. Polarization and anisotropy induced in the microwave background by cosmological gravitational waves. *Astron. Zh*, 62:1041–1052, 1984.

[88] A. Riess and A. Filippenko. Observational Evidence from Supernovae for an Accelerating Universe and a Cosmological Constant. *Astrophys. J.*, 116:1009–1038, 1998.

[89] V.A. Rubakov and P.G. Tinyakov. Infrared-modified gravities and massive gravitons. *Phys. Usp.*, 51:759–792, 2008.

[90] R. Sachs and A. Wolfe. Perturbations of a Cosmological Model and Angular Variations of the Microwave Background. *Astrophys. J.*, 147:73, 1967.

[91] Fulvio Sbisa, Gustavo Niz, Kazuya Koyama, and Gianmassimo Tasinato. Characterising Vainshtein Solutions in Massive Gravity. *Phys. Rev.*, D86:024033, 2012.

[92] Uros Seljak and Matias Zaldarriaga. A Line of sight integration approach to cosmic microwave background anisotropies. *Astrophys. J.*, 469:437–444, 1996.

[93] Uros Seljak and Matias Zaldarriaga. Signature of gravity waves in polarization of the microwave background. *Phys. Rev. Lett.*, 78:2054–2057, 1997.

[94] Fabio P Silva and Kazuya Koyama. Self-Accelerating Universe in Galileon Cosmology. *Phys. Rev.*, D80:121301, 2009.

[95] Stefan Sjors and Edvard Mortsell. Spherically Symmetric Solutions in Massive Gravity and Constraints from Galaxies. *JHEP*, 1302:080, 2013.

[96] L. Smolin. The Quantization of unimodular gravity and the cosmological constant problems. *Phys. Rev.*, D80:084003, 2009.

[97] Rafael D. Sorkin. Space-time and causal sets. 1990.

[98] Adamantios Stavridis and Clifford M. Will. Bounding the mass of the graviton with gravitational waves: Effect of spin precessions in massive black hole binaries. *Phys. Rev.*, D80:044002, 2009.

[99] Patrick J. Sutton and Lee Samuel Finn. Bounding the graviton mass with binary pulsar observations. *Class. Quant. Grav.*, 19:1355–1360, 2002.

[100] K. S. Thorne. Multipole Expansions of Gravitational Radiation. *Rev. Mod. Phys.*, 52:299–339, 1980.

[101] K. S. Throne. Relativistic radiative transfer:moment formalism. *Mon. Not. R. astr. Soc.*, 194:439–473, 1981.

[102] W. G. Unruh. A Unimodular Theory of Canonical Quantum Gravity. *Phys. Rev.*, D40:1048, 1989.

[103] A.I. Vainshtein. To the problem of nonvanishing gravitation mass. *Phys. Lett.*, B39:393–394, 1972.

[104] H. van Dam and M.J.G. Veltman. Massive and massless Yang-Mills and gravitational fields. *Nucl. Phys.*, B22:397–411, 1970.

[105] P. Van Nieuwenhuizen. On ghost-free tensor lagrangians and linearized gravitation. *Nucl. Phys.*, B60:478–492, 1973.

[106] Mikhail S. Volkov. Hairy black holes in theories with massive gravitons. *Lect. Notes Phys.*, 892:161–180, 2015.

[107] S. Weinberg. The Cosmological constant problems. *Talk given at Conference: C00-02-23, Proceedings.*

[108] Clifford M. Will. Bounding the mass of the graviton using gravitational wave observations of inspiralling compact binaries. *Phys. Rev.*, D57:2061–2068, 1998.

[109] Clifford M. Will. The Confrontation between General Relativity and Experiment. *Living Rev. Rel.*, 17:4, 2014.

[110] V.I. Zakharov. Linearized gravitation theory and the graviton mass. *JETP Lett.*, 12:312, 1970.

[111] Matias Zaldarriaga and Uros Seljak. An all sky analysis of polarization in the microwave background. *Phys. Rev.*, D55:1830–1840, 1997.

[112] Matias Zaldarriaga and Uros Seljak. Gravitational lensing effect on cosmic microwave background polarization. *Phys. Rev.*, D58:023003, 1998.

Vita

I went to Shandong University in China in the year of 2002. My major was optics engineering. I got my bachelor's degree of engineering in 2006. I came to the University of Mississippi in the United states to study theoretical physics in 2007. I received my master's degree of science in 2012 and Doctor's degree of philosophy in 2014.